

ON THE OPERATIONAL PREDICTABILITY OF BLOCKING

Stefano Tibaldi(*) and Franco Molteni
European Centre for Medium-range Weather Forecasts
Reading, United Kingdom

ABSTRACT

The entire seven year ECMWF operational analysis and forecast archive data is used to assess the skill of the Centre's model in short and medium range forecasting of atmospheric blocking. The assessment covers seven 100-day periods, from December 1 to March 10 of all winters from 1980-81 to 1986-87 inclusive. A slightly modified version of the Lejenas and Okland (1983) objective zonal index is used to quantify both observed and model forecast occurrence of blocking. The study is performed on 500mb geopotential height and on Euro-Atlantic and Pacific blocking separately. It is found that the model is, on average, more skilful if the initial conditions are blocked, but blocking onset is poorly represented if it occurs more than a few days into the forecast. This inability in entering the blocking regime has a substantial impact on the systematic error of the model.

(*) Current Address: Universita' di Bologna, Dipartimento di Fisica,
Via Irnerio 46, 40126 Bologna, ITALY

1. INTRODUCTION

Atmospheric blocking has long been recognized as a physical process of profound dynamical interest and of great practical relevance to operational forecasting. The crucial role that the onset, development and decay of block-like structures have on atmospheric low-frequency variability, and therefore on short, medium and long range forecasting, has made blocking one of the most studied atmospheric processes. For a review of recent observational, theoretical and numerical work on blocking, the reader is referred to Hollingsworth et al. (1987) and to Benzi et al. (1986a and 1986b).

Regarding the ability of numerical models to represent blocking, a few studies have been performed on long model integrations in order to assess the incidence of blocking in comparison with observed frequencies, duration and preferred locations, e.g. Mansfield (1984), Lau (1983). In order to perform such comparisons, the observational studies of Rex (1950), Dole and Gordon (1983), Lejenas and Okland (1983) and others have been used. Actual deterministic forecasting of blocking from observed initial conditions (as it is done in a routine numerical weather forecasting environment) has so far been even less documented, essentially because of the lack of a large homogeneous database of operational forecasts. Despite this lack of objective assessments of forecasting models' skill in representing blocking, there seems to be some sort of consensus among both modellers and synopticians on the fact that models perform slightly better during, and in the areas of, blocking than in situations of prevailing zonal flow (e.g. Persson, personal communication); but then persistence does the same, alas. Such feelings have also been quantified by synoptic evaluation of model performance during some individual blocking cases (see Bengtsson, 1981, Grønaas, 1982).

The European Centre for Medium-Range Weather Forecasts has now been producing and archiving operational analyses and medium-range forecasts for more than seven years; these archives make it now possible to try to quantify in a more objective way the ability of a state-of-the-art global forecasting model in representing blocking onset and maintenance. This is the purpose of this work. Section 2 describes, first of all, the database used for this study and the objective index that is used to determine whether or not a given analysis (or forecast) is considered to be blocked at a given longitude. Section 3 gives an overview of the overall model performance in representing blocking as

a function of longitude and in different years. Section 4 deals with the separate diagnosis of Euro-Atlantic and Pacific blocking, while Section 5 concentrates on blocking onset and blocking maintenance. Section 6 is devoted to the diagnosis of the model systematic error during different flow regimes and Section 7 gives a summary and attempts to draw some conclusions.

2. THE DATABASE AND THE DEFINITION OF AN OBJECTIVE BLOCKING INDEX

The database for this study is composed of all day 1 to 10 forecasts (and verifying analyses) of 500 mb geopotential height valid from December 1 to March 10 from 1980-81 to 1986-87 inclusive. Although each of the seven 100 day periods does not correspond exactly to the astronomical winter, we will refer to them as seven "winter" periods. All day 1 to 10 forecasts verify on the date of the corresponding analysis and are, therefore, initiated from different initial conditions (progressively lagging in time), in a way paralleling exactly the dataset used by Lorenz in his 1982 study (Lorenz, 1982). The complete dataset is therefore composed of 7700 fields (11 forecast times, including analysis time, 100 days per winter, 7 winter periods) projected on spherical harmonic coefficients truncated at triangular truncation 40 (T40). Although the original fields are global, we will restrict our analysis to the middle latitudes of the Northern Hemisphere, for which independent observational studies of blocking frequency on much larger datasets are available for the sake of comparison. One of the main limitations of this work (but by no means the only one) is due to the fact that the analysis was only carried out for a single season and at a single vertical level (500 mb). This is due to a variety of practical reasons, almost all having invariably to do with the amount of data to unload from the operational archives and to process further. There are plans to extend such analysis firstly to other periods of the year and then to other levels (and perhaps to the other hemisphere as well, if time and resources will permit). Another important limitation of our work is connected to the fact that the operational ECMWF General Circulation Model (GCM) has undergone several changes during the period here considered, many of which of major importance, be they of numerical nature (grid-point versus spectral technique or horizontal and vertical resolution) or of physical nature (parametrization of moist convection, vertical and horizontal diffusion and orographic effects). This limitation cannot be practically avoided if we want to have at our disposal a dataset of considerable size. Had we limited ourselves to a single period during which the model has remained fairly stable in its characteristics, the statistical significance of our results (already very limited with a total dataset composed of 700 days) would have been negligible.

In any objective study of atmospheric blocking, one of the main difficulties is to devise an objective method to determine whether a given flow pattern is

blocked or not at a certain point (or over a certain area) at a given moment in time (or over a certain period of time). This is related to the fact that no such thing as a typical block exists and the Earth's atmosphere uses very many of its almost infinite degrees of freedom to realize a variety of "similar" but in fact quite diverse situations, all of them in some sense blocked. So, it is extremely difficult to define a method that will satisfy the personal criteria of any number (however small but greater than one) of experienced synopticians. This work is no exception to this rule but, in addition to the usual disclaimers, we would like to point out that our main goal is not to diagnose the statistics of observed blocking in its spatial and temporal details, but to compare analysed and forecast fields, after having projected them on a suitable indicator. We hope that many of the shortcomings and limitations of our choice of objective definition of blocking will be of little relevance when the indicator is used in this "comparison mode". We will try to point out those results that might be most affected by the particular nature of the indicator.

We will, first of all, give here a local and instantaneous definition of blocking and later, in Section 4, generalise this to take into account longitudinal extension and time duration. This definition is essentially derived from the work of Lejenas and Okland (1983) to which the reader is referred for a more extensive justification of the criteria, not dissimilar to those used by Rex (1950). The procedure we have applied is as follows: the 500hPa field is firstly evaluated on a 4° by 4° regular latitude-longitude grid covering the Northern Hemisphere. Then the geopotential height gradients GHGS and GHGN are computed for each longitude point of the grid:

$$GHGS = (Z(\phi_o) - Z(\phi_s)) / (\phi_o - \phi_s)$$

$$GHGN = (Z(\phi_n) - Z(\phi_o)) / (\phi_n - \phi_o)$$

where:

$$\phi_n = 80^\circ N + \Delta$$

$$\phi_o = 60^\circ N + \Delta$$

$$\phi_s = 40^\circ N + \Delta$$

and $\Delta = -4^\circ, 0^\circ \text{ or } 4^\circ$

A given longitude is then defined as "blocked" at a specific instant in time if the following conditions are satisfied for at least one value of Δ :

(1) $\text{GHGS} > 0$ and

(2) $\text{GHGN} < -10$ m/deg lat

We decided to restrict Lejenas and Okland's criterion (that is essentially equivalent to condition (1) alone) because we found that the addition of condition (2) was successfully eliminating from the "blocking catalogue" situations of large southward displacement of the midlatitude westerly jet that marginally satisfy condition (1) but not condition (2) and that, synoptically, would not be generally recognized as blocked.

3. THE OVERALL MODEL PERFORMANCE IN REPRESENTING BLOCKING

We will start by showing the behaviour of the objective (local and instantaneous) index as a function of longitude. Fig. 1 shows the percentage frequency of blocking (objectively defined as above) as a function of longitude and computed on all ECMWF daily objective analyses of our database. Remembering that we have restricted our analysis to the Winter period, this figure can be compared with Fig. 3 of Lejenas and Okland (1983), showing that our modified version of their index behaves in a very similar way as far as the dependency on longitude is concerned. The two well known maxima of frequency in the Euro-Atlantic and Pacific regions are well reproduced and a further secondary maximum around 50°E is also noticeable, associated with the relatively (and synoptically well known) frequent occurrence of Euro-Asian blocks. The two shaded regions also appearing in the figure will be used later in Section 4 to define objectively the concept of "blocked sector".

Figure 2 shows again the same diagram of Figure 1, but superimposed onto the corresponding diagram computed on the forecast fields, for Day 1, 3, 6 and 10 (panels a to d respectively). This comparison allows us to document the progressive degradation of the performance of the operational forecasts for increasing forecast time. This degradation appears as a progressive loss of the amplitude of the two main blocking frequency maxima until, by Day 10, the forecast maxima show approximately one half of the observed amplitude and also fairly appreciable phase shifts; more specifically, the Euro-Atlantic maximum has been shifted eastward by approximately 20°, while the Pacific maximum has been shifted westward by an even greater quantity, approximately 40° to 50°.

Such model behaviour is quite consistent with the well known deficiencies of general circulation models in general (and of the ECMWF GCM in particular). It has in fact been well documented (e.g. Hollingsworth et al., 1980; Bengtsson and Simmons, 1982; Wallace et al., 1983; Bettge, 1983; Arpe and Klinker, 1986; Palmer et al., 1986; Tibaldi et al., 1987) that GCMs tend to move, with increasing integration time, towards a climate "of their own" with increased mid latitude westerlies and decreased amplitude of planetary scale quasi-stationary waves. A variety of hypotheses have been put forward as to the possible causes for such behaviour (representation of mountains, horizontal and vertical diffusion, parametrization of convection etc., see

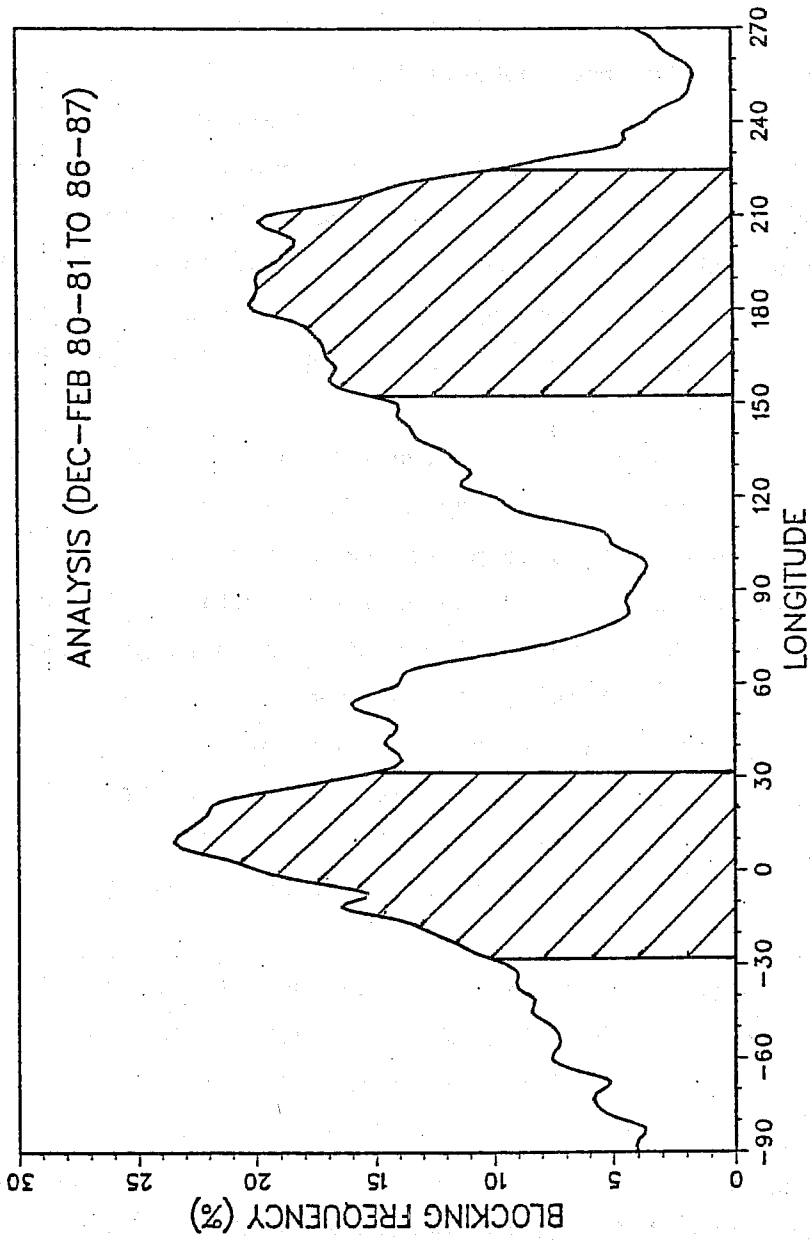


Fig. 1 Percentage frequency of blocking (objectively defined in Section 2) as a function of longitude and computed on all ECMWF daily objective analyses of our database.

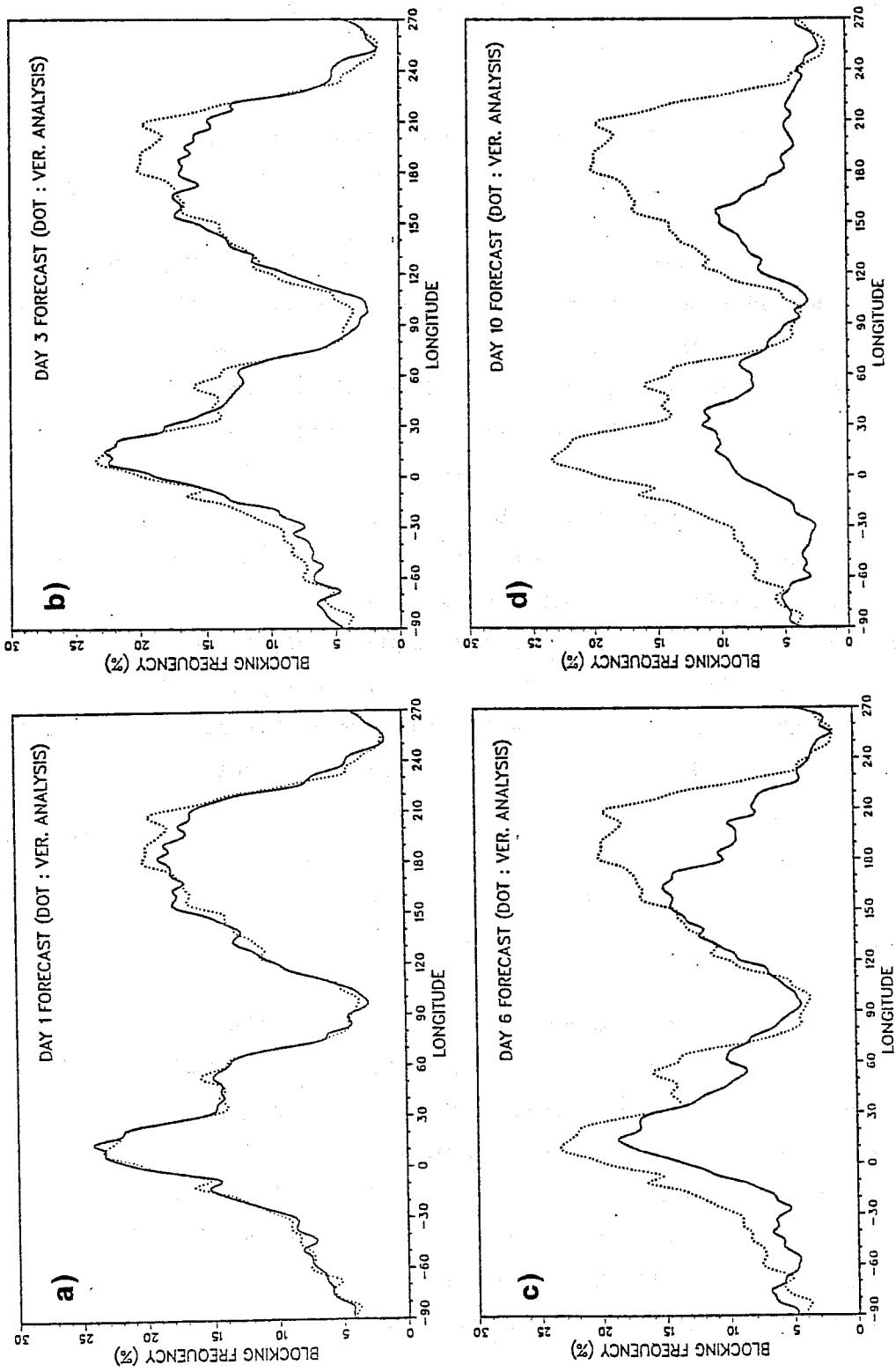


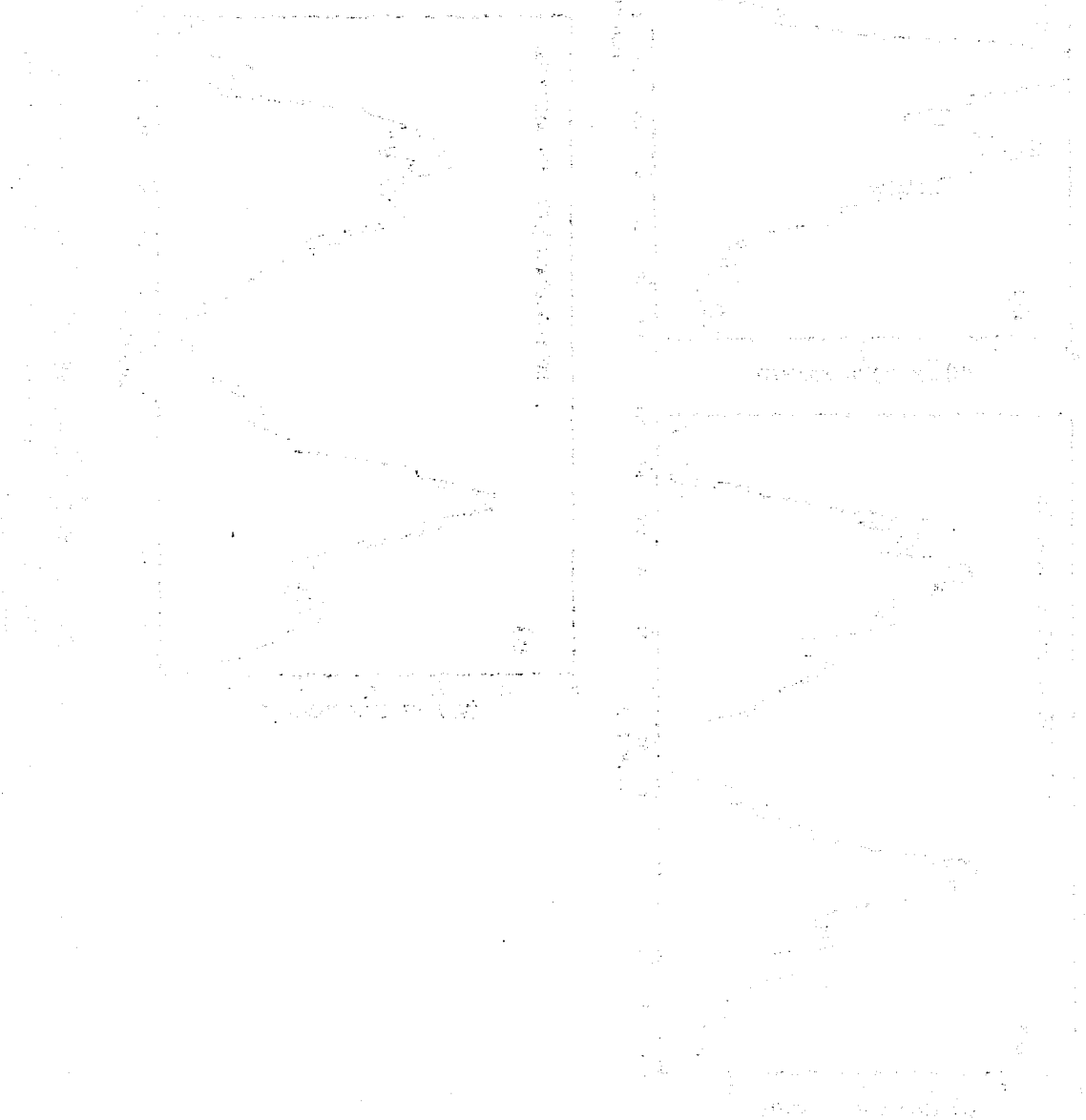
Fig. 2 Dotted lines: as in Figure 1. Full lines: blocking frequency computed on the forecast fields, for Day 1, 3, 6 and 10 (panels (a) to (d) respectively).

many of the works quoted above), but the fact remains that such a model-produced climate is consistent with the apparent inability of the ECMWF GCM to reproduce the observed blocking frequency maxima at the proper longitudes. We will comment further in Section 6 on this fact when we will analyze the relationships between representation of blocking and model Systematic Errors.

We now want to investigate, within the limitations imposed by the dataset at our disposal, whether the main model changes that have taken place during the period considered here have had an impact on the ability of the operational forecasting system to represent blocking. Of course, this man-produced variability of the model performance overlaps and interacts with the natural year-to-year variability of blocking frequency and of circulation types. We will show diagrams similar to those of Fig. 2 for three separate two-winter periods: 1981-82 and 82-83; 83-84 and 84-85; 85-86 and 86-87. In the first period the operational model was an N48 grid-point model (48 grid-points between poles and equator) with a grid-box-mean orography. In the second period the model was a T63 spectral model (triangular truncation at wavenumber 63) with a $\sqrt{2}$ sigma envelope orography (Wallace et al., 1983), and in the third period a T106 spectral model with a 1 sigma envelope orography. We decided to exclude the first winter (1980-81) from this particular stratification of the analysis, because the model was at a preliminary stage of development and the model orography was excessively smooth, in addition, this orography was used in a one winter period only, while all the other three periods cover two winters. Figures 3 to 6 show graphs similar to those of Fig. 2 but for the three two-winter periods separately (panels a to c) and for forecast days 1,3,6 and 10 (Fig. 3,4,5 and 6 respectively).

The first consideration we should make is that a large interannual variability is evident, with the second two-winter period showing an anomalously high frequency of those Euro-Asian blocked situations mentioned above. Their almost complete absence from the other two periods makes it obvious that the secondary maximum of frequency apparent in Fig. 1 around 50°E is almost completely due to episodes taking place during the winters of 1983-4 and/or 1984-85. Secondly, it is evident that the model's inability to represent blocking at an advanced stage during the forecast is not confined to any

particular winter and has improved little with time and model development. The only notable exception to this is medium-range (day 6) Euro-Atlantic blocking during the third two-year period (Fig. 5c), apparently much better represented than in other periods for the same forecast time. Unfortunately, our sample is insufficient to substantiate this statistically, and in fact a similar behaviour can be seen in Fig. 5a for Pacific blocking. Since this panel refers to an old version of the model (that hopefully has been improved upon since then), we must conclude that both these episodes of variability in model performance might be due to poor sampling, rather than to systematic differences in model ability.



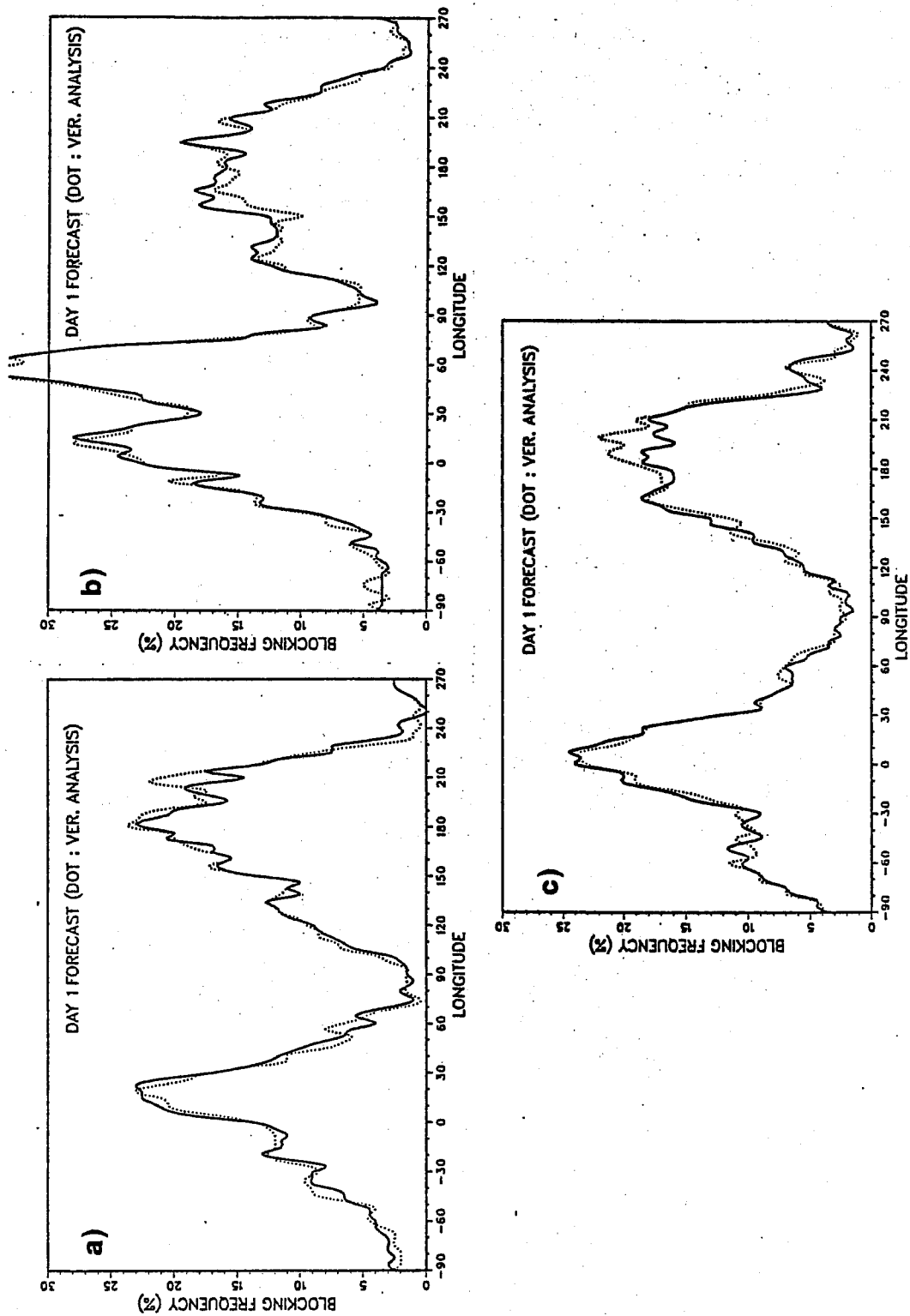


Fig . 3 As in Fig. 2, but for forecast day 1 only and for 3 two-winter periods separately: a) 1981/82 and 1982/83; (b) 1983/84 and 1984/85; (c) 1985/86 and 1986/87.

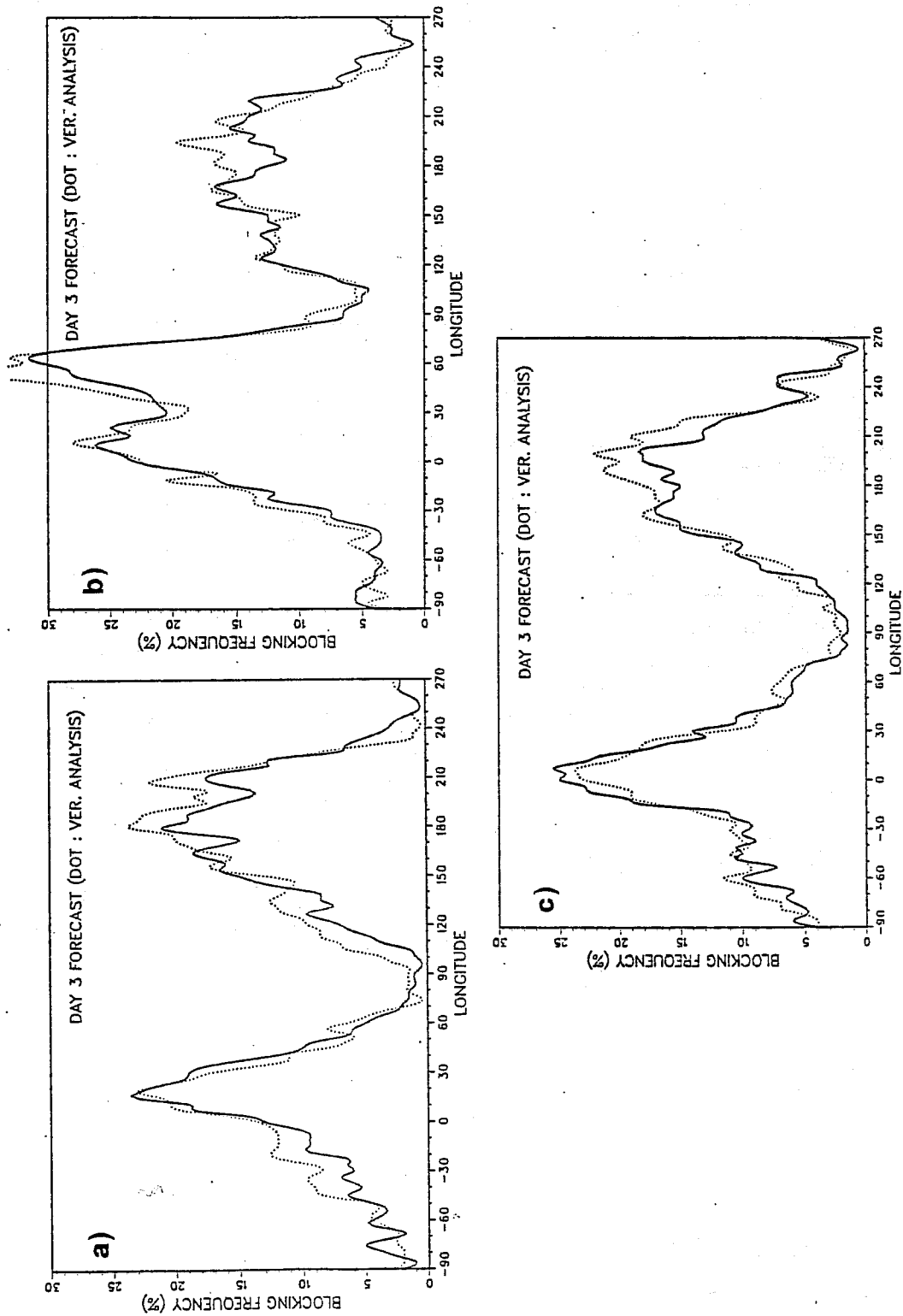


Fig. 4 As in Fig. 3, but for forecast day 3.

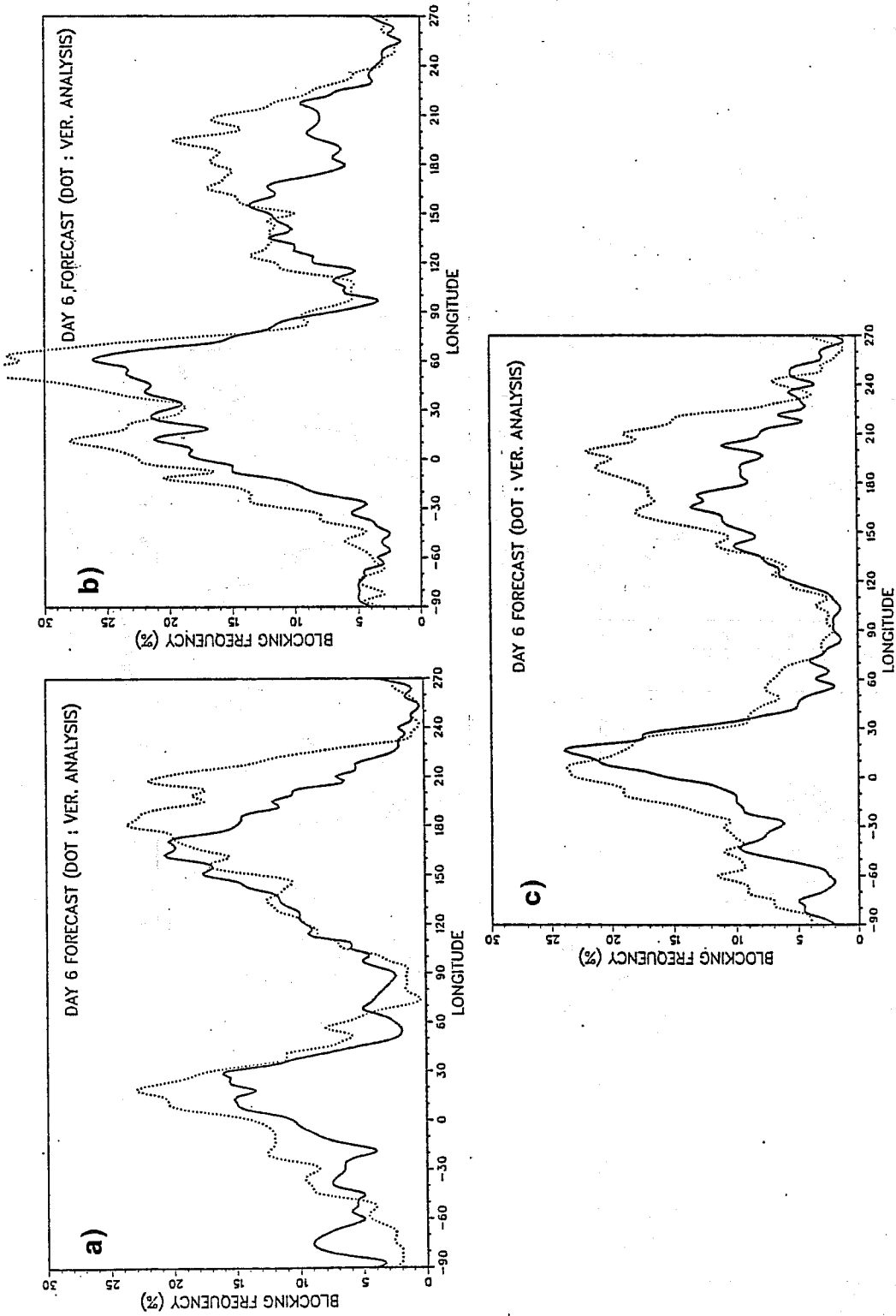


Fig. 5 As in Fig. 3, but for forecast day 6.

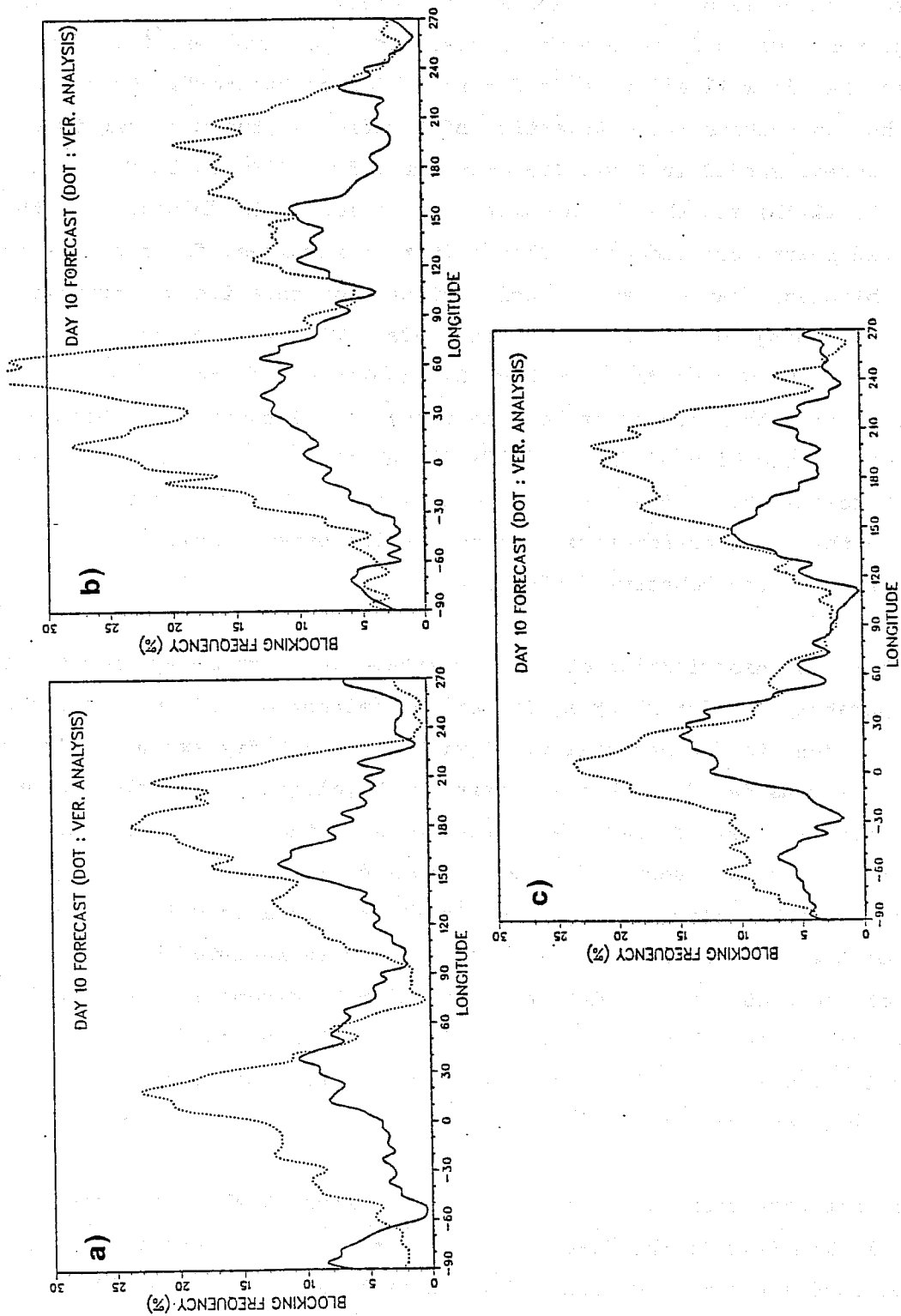


Fig. 6 As in Fig. 3, but for forecast day 10.

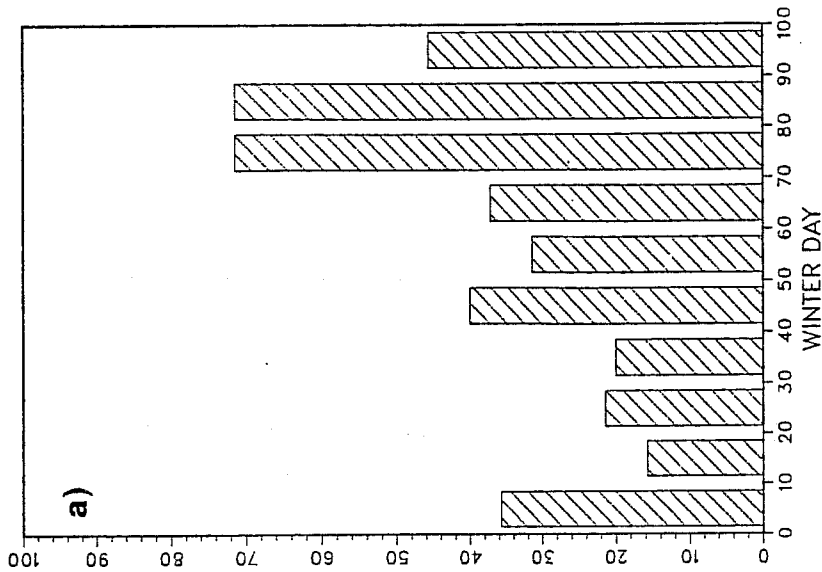
4. EURO-ATLANTIC AND PACIFIC BLOCKING

So far we have only very broadly examined the model's ability to represent local and instantaneous blocking conditions as defined by our objective index, as a function of longitude and forecast time. We want now to be able to distinguish between Euro-Atlantic and Pacific blocking in such an analysis. For this purpose, we need to develop further our objective definition of blocking so that it will allow us to define a blocked "sector". We do so by defining the two sectors (Euro-Atlantic and Pacific) as the two longitude bands that appear shaded in Fig.1 (Euro-Atlantic from 28°W to 32°E and Pacific from 152°E to 224°E) and then by assuming that a sector is "blocked" if three adjacent grid points are blocked. This criterion requires, for a sector to be considered blocked, that we have a region of zero or negative geostrophic westerlies extending for at least 12° longitude. With this criterion, on a total number of 700 Winter days, we have 278 unblocked ("zonal") days, 422 blocked days (in either one or in both sectors), 273 Euro-Atlantic blocked days and 285 Pacific blocked days. $(273+285)-422=136$ is the number of days with both Euro-Atlantic and Pacific sectors blocked. Before turning our attention to the model performance, let us examine briefly some characteristics of the "observed" blocking.

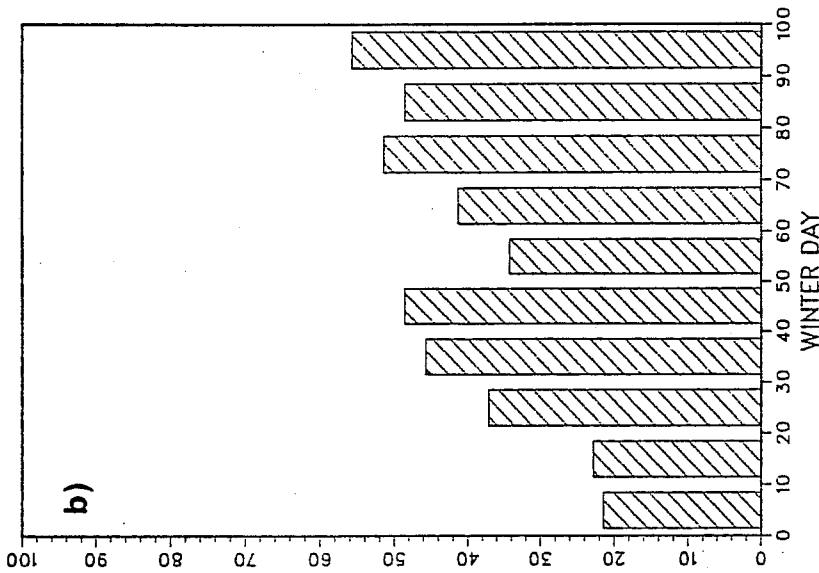
Figure 7 shows the distribution of the percentage of blocked days for the two sectors separately and for blocking in general (either one of the two sectors blocked) as a function of seasonal time (within the 100 day extended winter period we have considered). This is useful to highlight a possible seasonal trend, if there is one. Indeed the histograms show that the probability to have blocking (in either sector) increases considerably with time. Figure 8, conversely, shows how blocking days are distributed as a function of the amplitude of the block itself, at least as this is represented by the amplitude of the GHGS gradient defined in Section 2 (essentially proportional to the strength of the geostrophic easterlies). Intense Pacific blocks appear to be relatively more probable than their Euro-Atlantic counterparts; the reverse is true for very weak blocks.

Turning now our attention to model performance, Figure 9 shows the total number of blocked days in the forecast for the two separate sectors, as a function of forecast time. Forecast day 0 indicates the analyzed ("observed") values. The shaded portion of the histograms bars indicates the contribution

PERCENTAGE OF BLOCKING DAYS — EURO ATLANTIC BL.



PERCENTAGE OF BLOCKING DAYS — PACIFIC BL.



PERCENTAGE OF BLOCKING DAYS — E.A. + PAC.

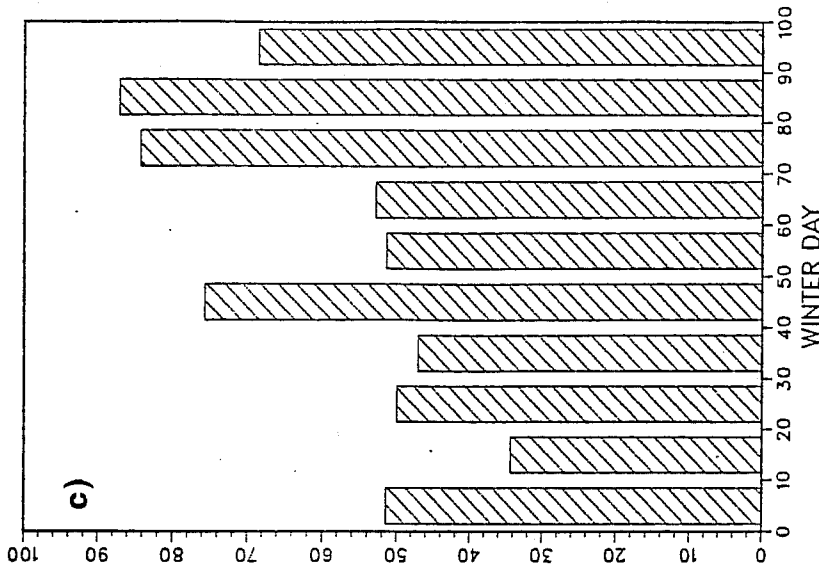
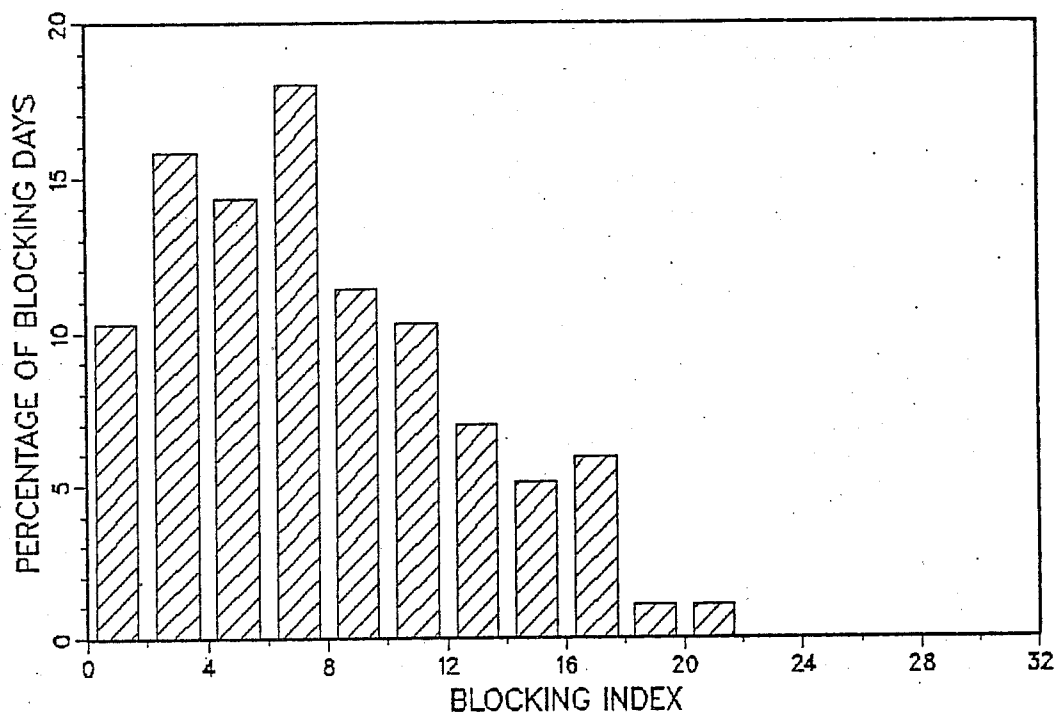


Fig. 7 Percentage of blocked days for the Euro-Atlantic sector (a), the Pacific sector (b) and for blocking in general (either one of the two sectors blocked) (c) as a function of seasonal time (within the 100-day winter period).

a) DISTRIBUTION OF OBSERVED BLOCKING INDEX – EURO ATLANTIC BL.



b) DISTRIBUTION OF OBSERVED BLOCKING INDEX – PACIFIC BL.

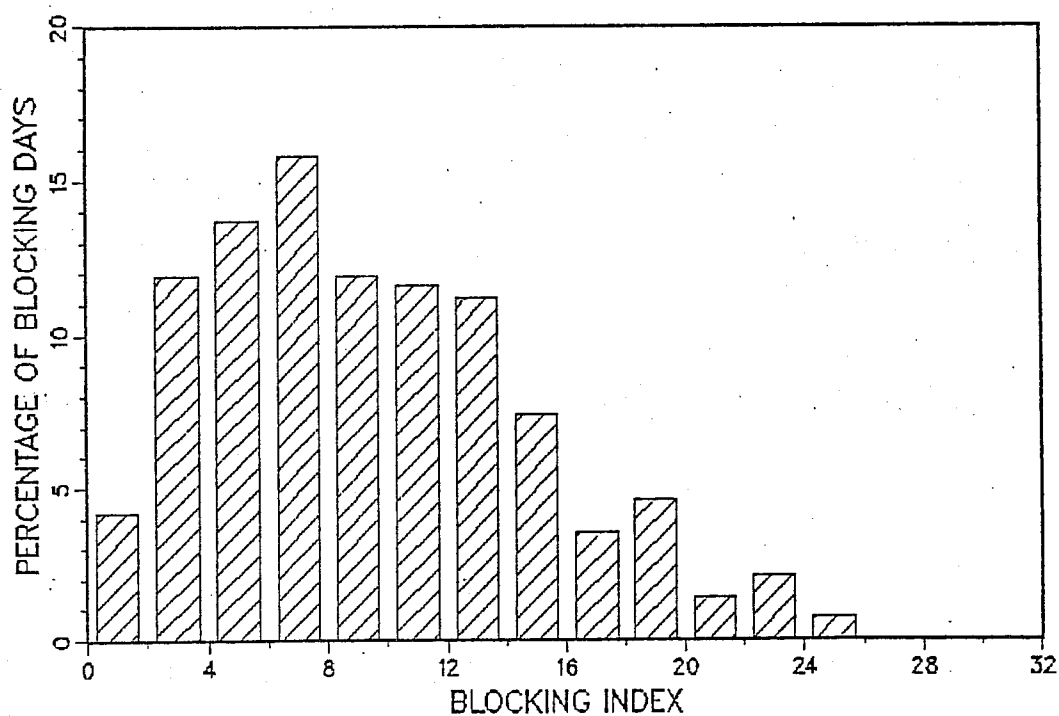
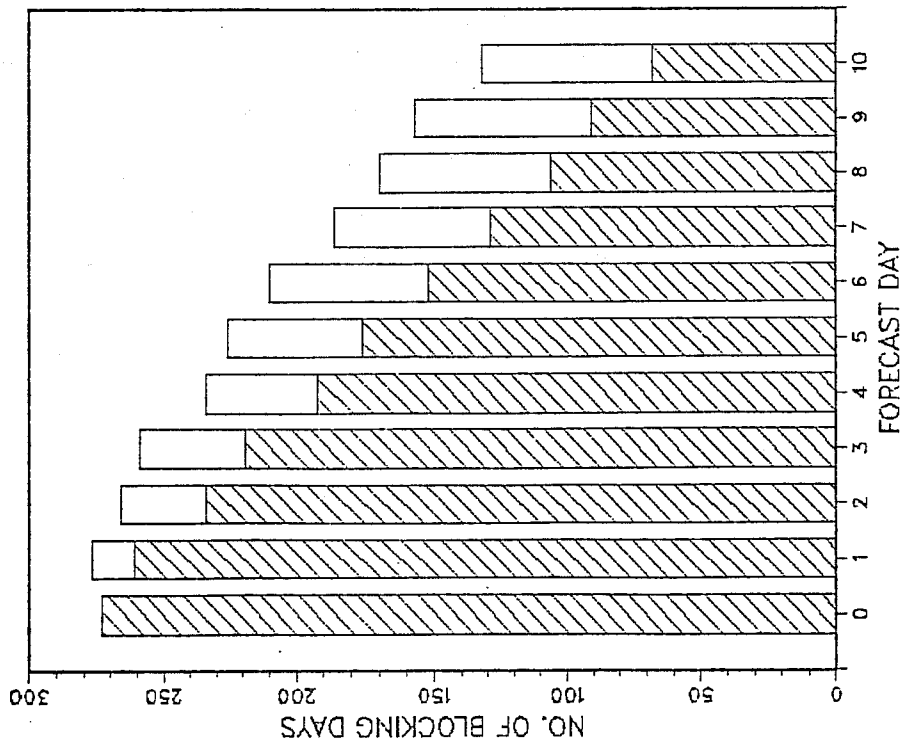


Fig. 8 Distribution of blocking days as a function of the amplitude of the block itself, as represented by the maximum value of the GHGS index (in m/deg); (a) Euro-Atlantic blocking; (b) Pacific blocking.

a) EURO-ATLANTIC BLOCKING



b) PACIFIC BLOCKING

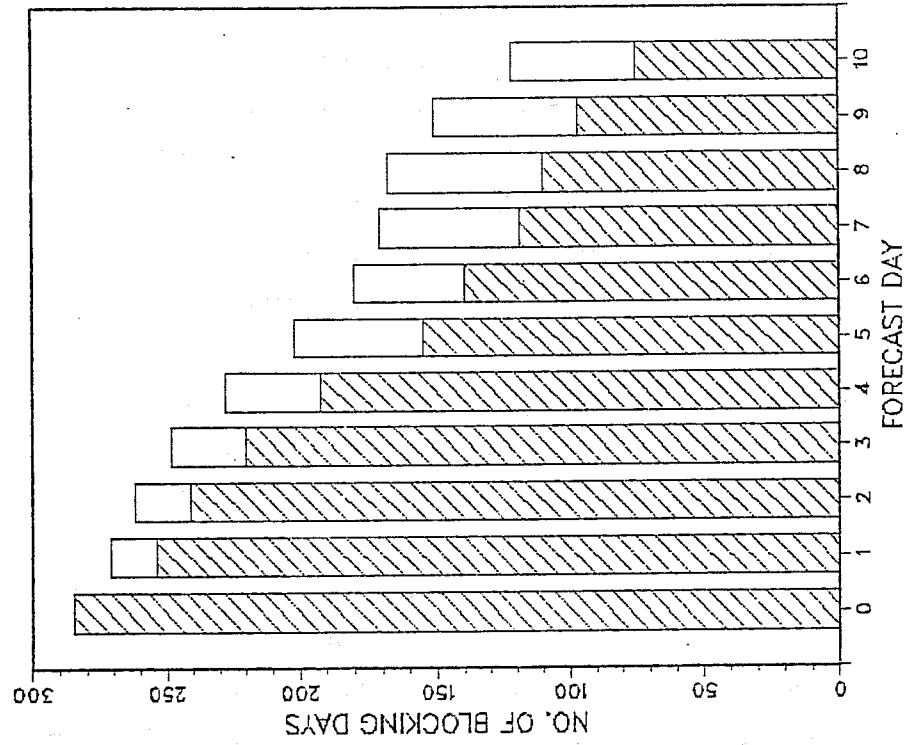
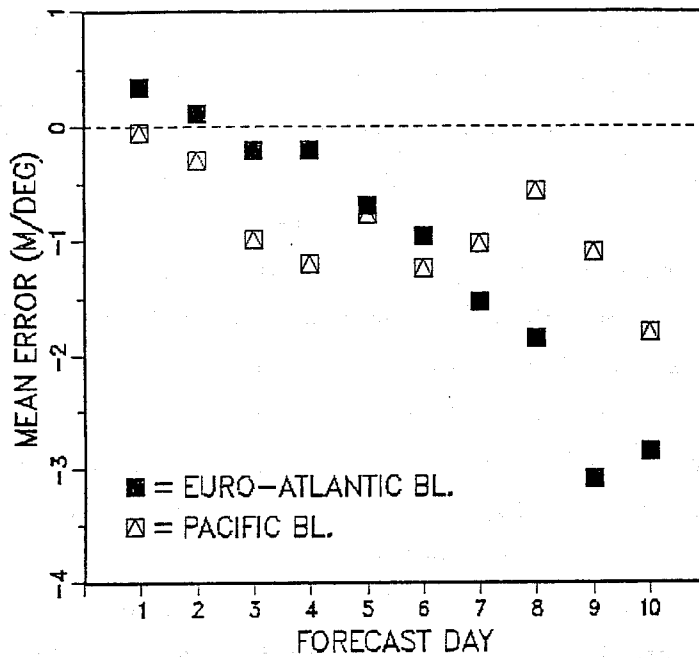


Fig. 9 Total number of blocked days in the forecast for the Euro-Atlantic (a) and the Pacific (b) sectors as a function of forecast time. Forecast day 0 indicates the analyzed values. The shaded portion of the bars indicates the number of days that are correctly forecast as blocked; the topmost blank part of the bars represents the days that are blocked in the forecast but not in the verifying analysis.

to the total from those days that are correctly forecast as blocked, while the topmost blank part of the bars indicates the contribution from those days that are erroneously forecast as blocked, i.e. that are blocked in the forecast but not in the verifying analysis. The main indication of the results shown in Fig. 9 is that, by Day 10, the forecasts for the Euro-Atlantic sector are blocked in a number of days that is only 50% of the observed total (see, for example, also Fig. 2d). However, half of the forecast blocked days are not verified by the corresponding analysis, leaving the total number of correct (verified) 10 day forecasts of blocking at only 25% of the observed. The situation for the Pacific sector is only marginally better, see Fig. 9b.

We are now interested in diagnosing whether the model, even in those cases for which it is correctly forecasting a blocked sector, does so with systematic amplitude and phase (longitude) errors. Our index allows such an estimate if we interpret the maximum value of the GHGS index (in units of geopotential meters per degrees latitude) in the blocked sector as a measure of the amplitude of the block and the longitude of this maximum as a measure of the phase. Figure 10 shows mean errors in the index value and in longitude (amplitude and phase errors) as a function of forecast time. Here we can confirm quantitatively what could already be qualitatively seen from Fig. 2: the model tends to shift Euro-Atlantic blocks progressively eastward, while it shifts the Pacific blocks westward (Fig. 10b). The model also loses amplitude in both sectors; but the amplitude loss seems to take place more rapidly in the case of Pacific blocks. (The apparent recovery in the mean errors that can be seen after day 7, especially in the case of Pacific blocking, is most likely due to the fact that only very persistent blocks are still detectable in the forecast after one week, so that the statistics displayed in Fig. 10 become representative only of the most predictable cases). Such differences of modelling characteristics are consistent with the hypothesis that the (at least partially) different physical mechanisms give the most relevant contribution to the maintenance of blocks in the two sectors.

a) MEAN ERROR IN BLOCKING INDEX



b) MEAN ERROR IN BLOCKING LONGITUDE

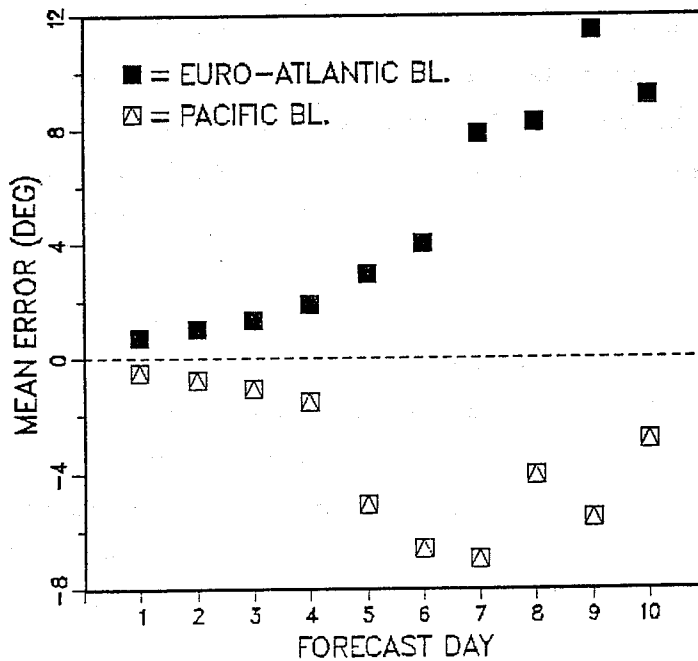


Fig. 10 Mean errors in the maximum value of the GHGS index (a) and in the corresponding longitude (b) (blocking amplitude and phase errors) as a function of forecast time.

5. MODELLING BLOCKING ONSET AND MAINTENANCE

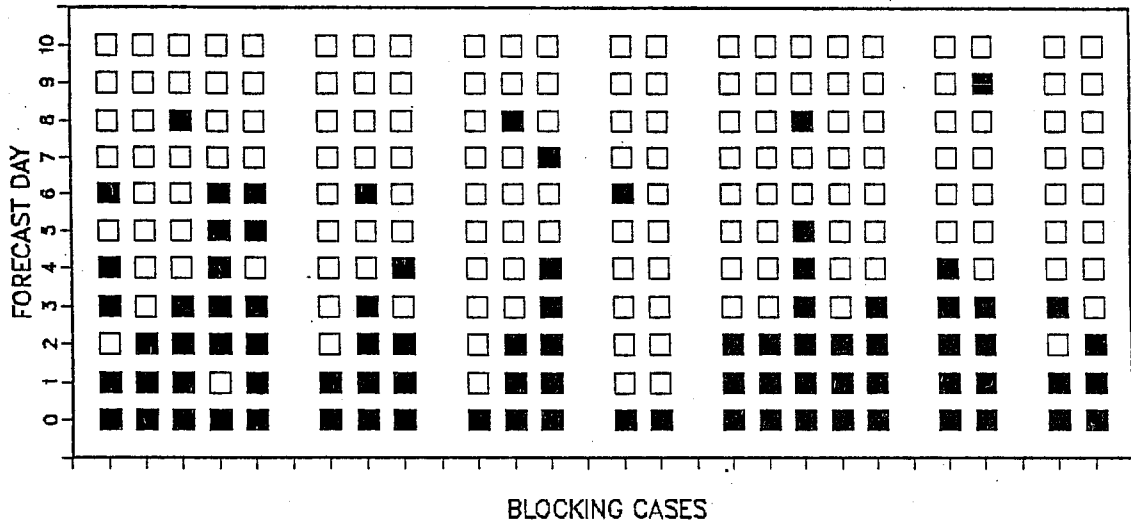
It is conceivable (and many theoreticians and synopticians have speculated along this line of thought) that different physical mechanisms are to be held responsible for blocking onset and for blocking maintenance. If blocking is indeed a metastable "state" (global or local is of little consequence, at this stage of the argument) which the atmosphere enters as a result of an instability mechanism (e.g. Charney and DeVore, 1979; Charney and Strauss, 1980; Källén, 1981; Malguzzi and Speranza, 1981; Speranza, 1986; Benzi et al., 1986a; Benzi et al., 1986b) then it should be a priori expected that during highly unstable situations (as immediately before and during the onset) numerical forecasting should be a daunting task; on the contrary in fairly stable conditions (as when a block is well established) forecasting should be a more tractable problem. It is, in fact, a widespread belief that numerical models have, in general, more difficulties in entering a blocked situation than they have in maintaining a block once this is already present in the initial conditions from which the integration is started. We want now to address this problem by analysing separately blocking onset and blocking maintenance and the model's ability at reproducing both. To do this we need once more to restrict our definition of blocking in order to be able to define "episodes" objectively; in a very simple and straightforward manner we decided to define a "blocking episode" when a sector is blocked for at least four consecutive days according to the observed date. With this definition, we found 22 cases of Euro-Atlantic and 24 cases of Pacific blocking in our 700 days dataset. We shall now concentrate on blocking onset first.

Figure 11 attempts to show the model's ability to forecast blocking onset. Each of the 22 Euro-Atlantic (panel a) and 24 Pacific (panel b) cases is represented by one column. A black square at forecast day n indicates that the forecast verifying on the first day of the blocked period (the blocking "onset") and started n days before was also blocked according to our criterion; a hollow square indicates a failure. Obviously, all squares are black at forecast day 0 (the analysis) and most of them are black at forecast day 1, indicating that very short-range forecast of blocking onset is fairly successful (not completely, however; on a total of $22+24=46$ cases, 8 failed, although in 4 such failures some previous longer-range forecasts had given the correct indication). The general picture is one of some almost complete failures, some (less, however) outstanding successes and many ordinary cases

in which the forecast gives good guidance up to three to four days in advance. There seems to be, this time, no obvious and systematic difference of model behaviour between the two sectors and also no obvious trend in model performance from winter to winter (the cases belonging to different years are grouped together and time increases from left to right). The overall results are somewhat disappointing but we would like to remind the reader that it is highly likely that a good synoptician can extract useful guidance from the forecast maps even for some of those cases that have been penalized by the objective indicator. In fact, if our criterion is only marginally satisfied by the analysis, even a small difference in the circulation pattern can affect the classification of the forecast. To test the sensitivity of our objective definition of onset we have computed the same diagrams of Fig. 11, but for the second day of each blocking episode (Figure 12). Indeed the performance of the forecasting model appears to be better in this case, which is partially due to the stronger blocking signature but also to the fact that the initial conditions are one day closer to the actual onset for a given forecast time.

To summarize the results on the diagnostics of forecast of blocking onset we present the histograms of Figure 13. Each panel gives the number of cases of blocking onset correctly forecast as a function of forecast lead time. For the first day of blocking, the model data appear to contain little useful information on the onset beyond forecast day 3, with very little difference between the two sectors. The impression received by comparing qualitatively Figs. 11 and 12 is here confirmed more quantitatively: forecasting the second day of blocking is measurably more successful than forecasting the first day: at forecast day 3 we have 11 successful predictions of the first day in the Euro-Atlantic sector against 16 good forecasts of the second day (on a total of 22 cases). The respective figures for the Pacific sector are 12 against 21 over a total of 24. In most cases, the day $n+1$ forecast of the second day of blocking is better than the day n forecast of the first day (these two forecasts come from the same model integration, started from the initial conditions analyzed n days before the onset of the block). For example, we have 13 and 15 good 4-day forecasts of the second day of the block against 11 and 12 3-day forecasts of the first day (Euro-Atlantic and Pacific sectors respectively). This indicates that transitions to blocking occur more slowly in the model than in the actual atmosphere.

a) FORECAST OF BLOCKING ONSET – FIRST DAY OF EURO-ATLANTIC BL.



b) FORECAST OF BLOCKING ONSET – FIRST DAY OF PACIFIC BL.

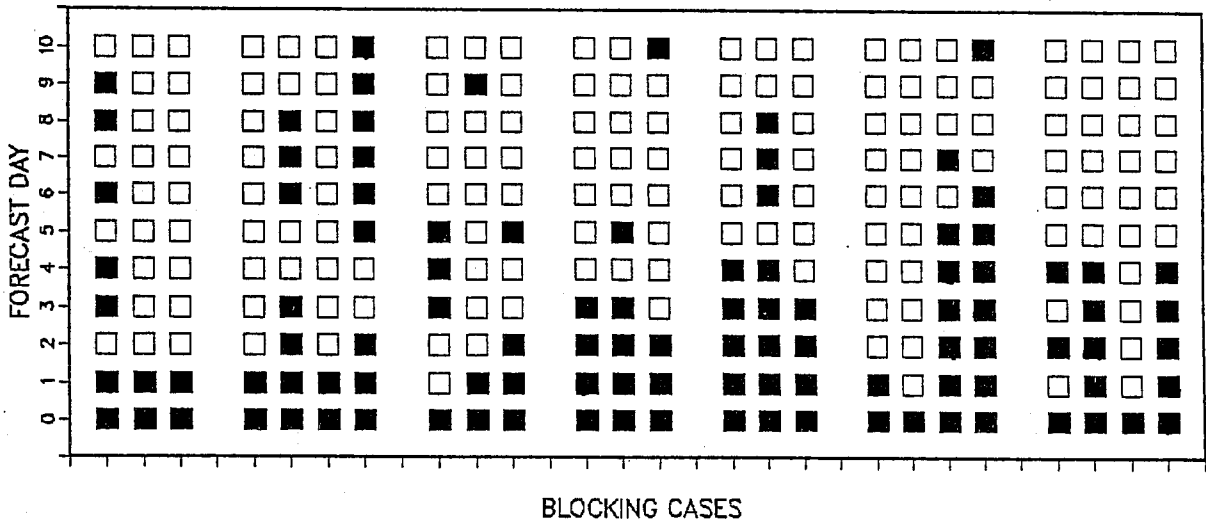
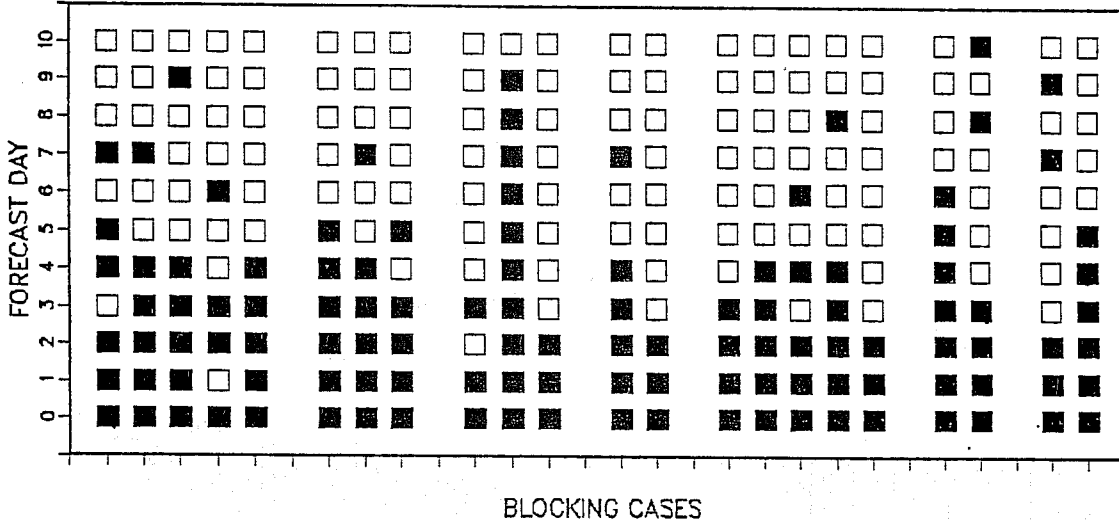


Fig. 11 Diagram of successful (black squares) and unsuccessful (hollow squares) forecasts of the observed blocked regime in the first day of each of 22 Euro-Atlantic (a) and 24 Pacific (b) blocking episodes, as a function of the forecast time. Cases belonging to the same winter are grouped together.

a) FORECAST OF BLOCKING ONSET – SECOND DAY OF EURO-ATLANTIC BL



b) FORECAST OF BLOCKING ONSET – SECOND DAY OF PACIFIC BL

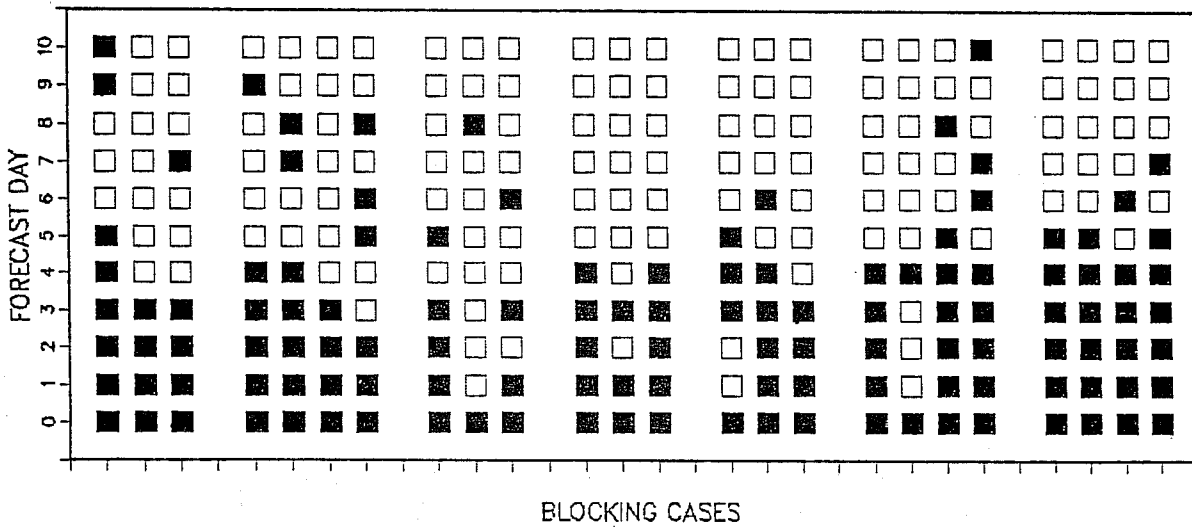


Fig. 12 As in Fig. 11, but for the second day of each blocking episode.

CORRECT FORECASTS OF BLOCKING ONSET

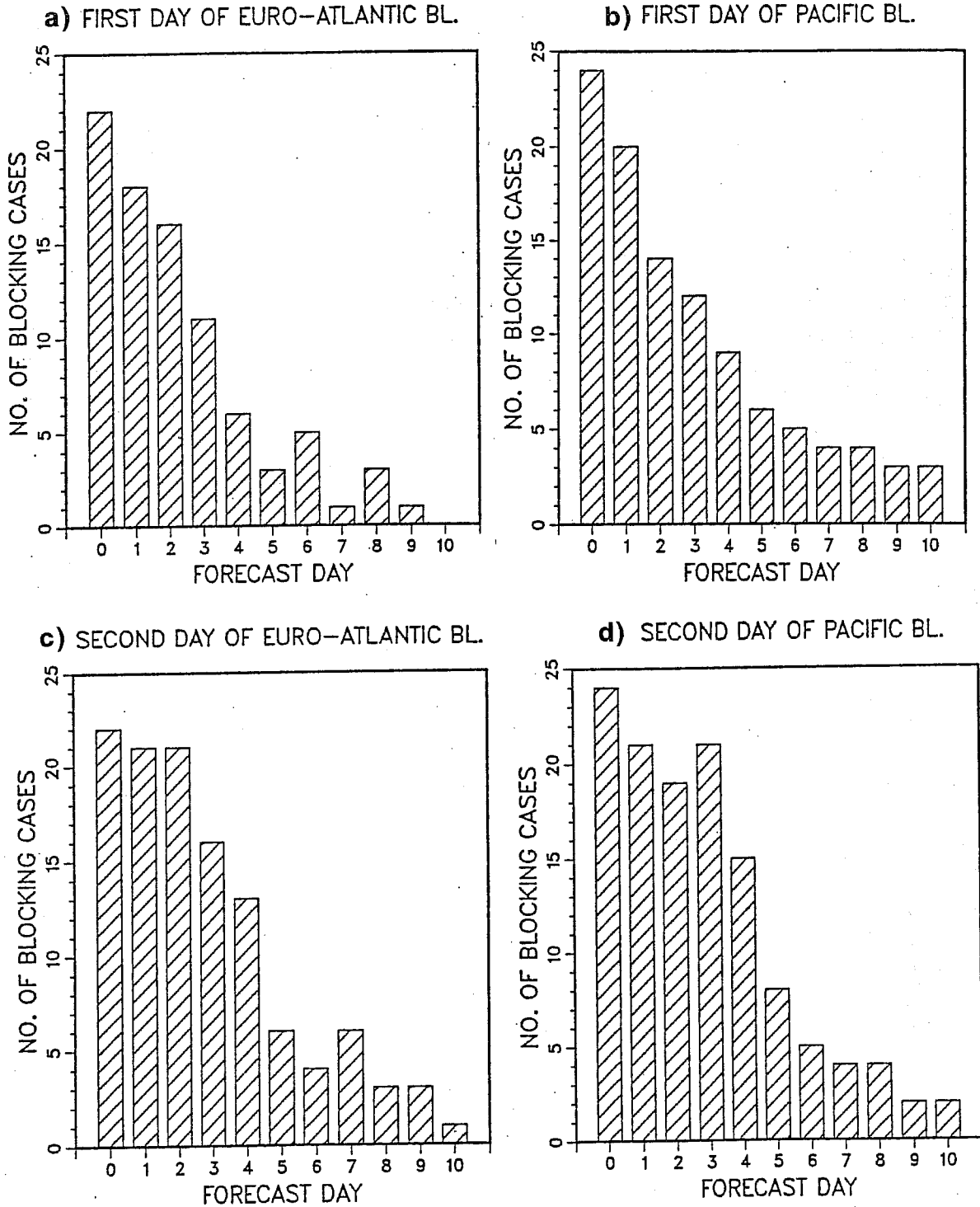


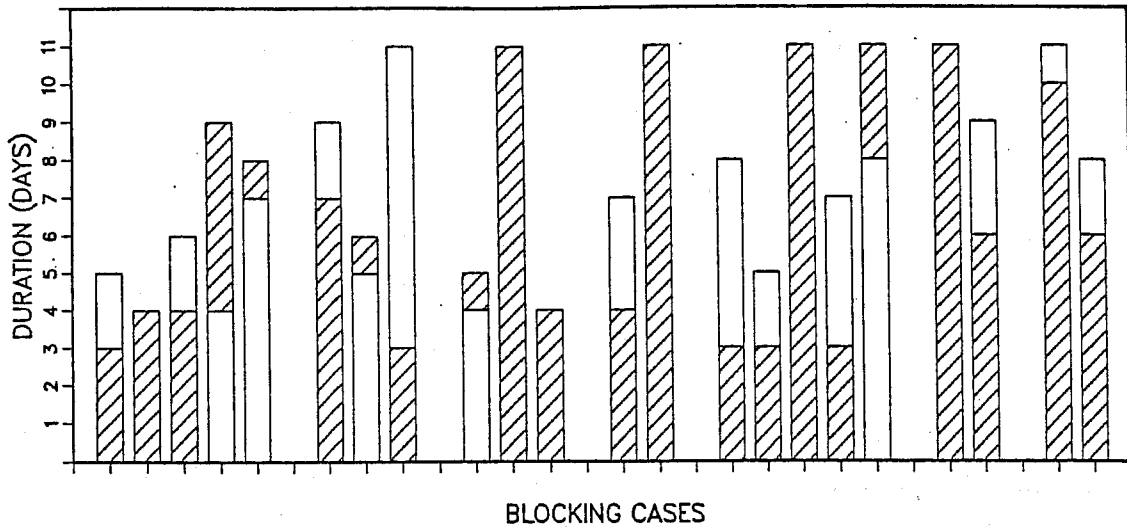
Fig. 13 Number of cases of blocking onset correctly forecast as a function of forecast lead time. Panels (a) and (b) refer to the first day of the blocking episodes, panels (c) and (d) to the second day. Panels (a) and (c) refer to Euro-Atlantic blocking, panels (b) and (d) to Pacific blocking.

We now move to blocking maintenance (or, more precisely, duration). We will now analyze all those forecasts that start from the first day of a blocking episode; therefore, from an initial condition that already contains a block in one of the two sectors under analysis. Figure 14 has the same general layout of Fig. 12, but now the vertical bars indicate both analysed and forecast duration (shaded and white bars, respectively). The cases are, of course, the same as for Fig. 12. So, if the topmost portion of the vertical bars is white, the forecast duration is longer than the observed. If the topmost part of the bars is shaded, the reverse is true. In case of a "perfect" forecast, the bar is completely shaded. A duration (either observed or forecast) of 11 days signifies a duration longer than 10 days.

The overall performance of the model appears to be fairly satisfactory; even if predicted blocks either shorter or longer than observed are quite common, a few outstanding successes in forecasting blocks longer than 10 days are apparent in both sectors. A closer look at the precise figures reveals that, on average, the model is in fact underestimating blocking duration; this is shown more clearly in Figure 15, where histograms of the number of cases as a function of duration are displayed for the two sectors separately, as usual. While no observed case shorter than four days is present (by definition of episode), respectively 5 and 4 cases of shorter blocks occur in the two sectors in the forecast. Conversely, the number of analysed blocks longer than 10 days is always higher than the corresponding forecast number (6 against 5 for the Euro-Atlantic and 10 against 4, a much larger error, for the Pacific sector).

The different skill of the model in forecasting the duration of long-lived blocks over the Euro-Atlantic and the Pacific sector again suggests the possibility of differences in the contribution of various physical processes to the maintenance of blocking in the two sectors. For example, the relevance of the transient eddy forcing mechanism proposed by Green (1977) has been clearly documented in a number of papers for the Atlantic blocking (see for example Illari and Marshall, 1983; Shutts, 1986; Hoskins and Sardeshmukh, 1987), but comparable evidence has not yet been provided for Pacific cases.

a) FORECAST OF BLOCKING DURATION – EURO ATLANTIC BL.



b) FORECAST OF BLOCKING DURATION – PACIFIC BL.

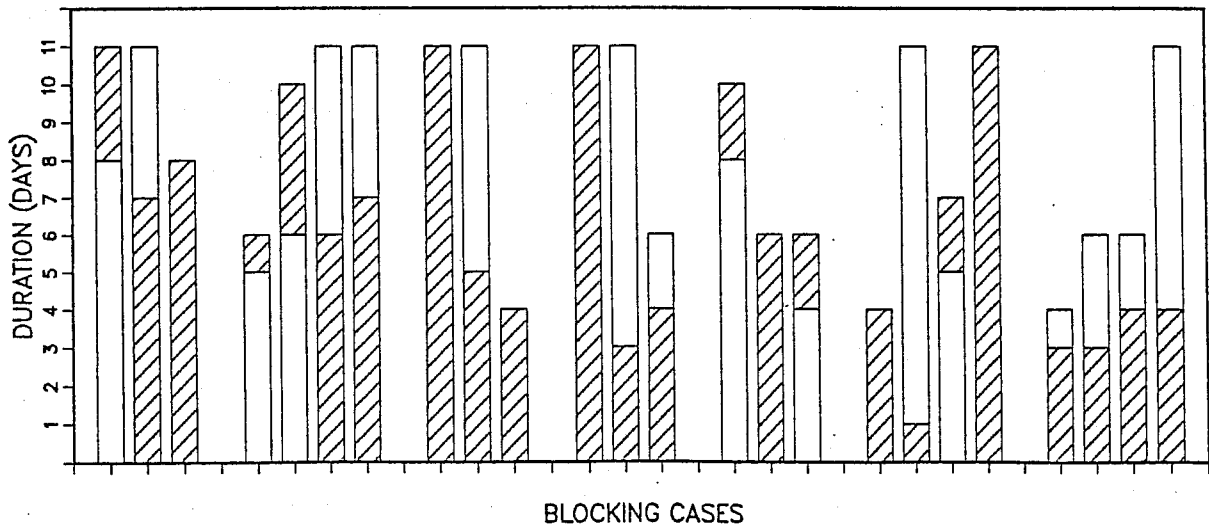


Fig. 14 Duration of the 22 Euro-Atlantic (a) and 24 Pacific (b) blocking episodes as deduced from the analysis (shaded bars) and from the forecast started on the first day of each episode (white bars). A duration of 11 days indicates any duration longer than 10 days. The white bar is fully covered by the shaded bar when the forecast duration equals the observed one.

DISTRIBUTION OF BL. DURATION

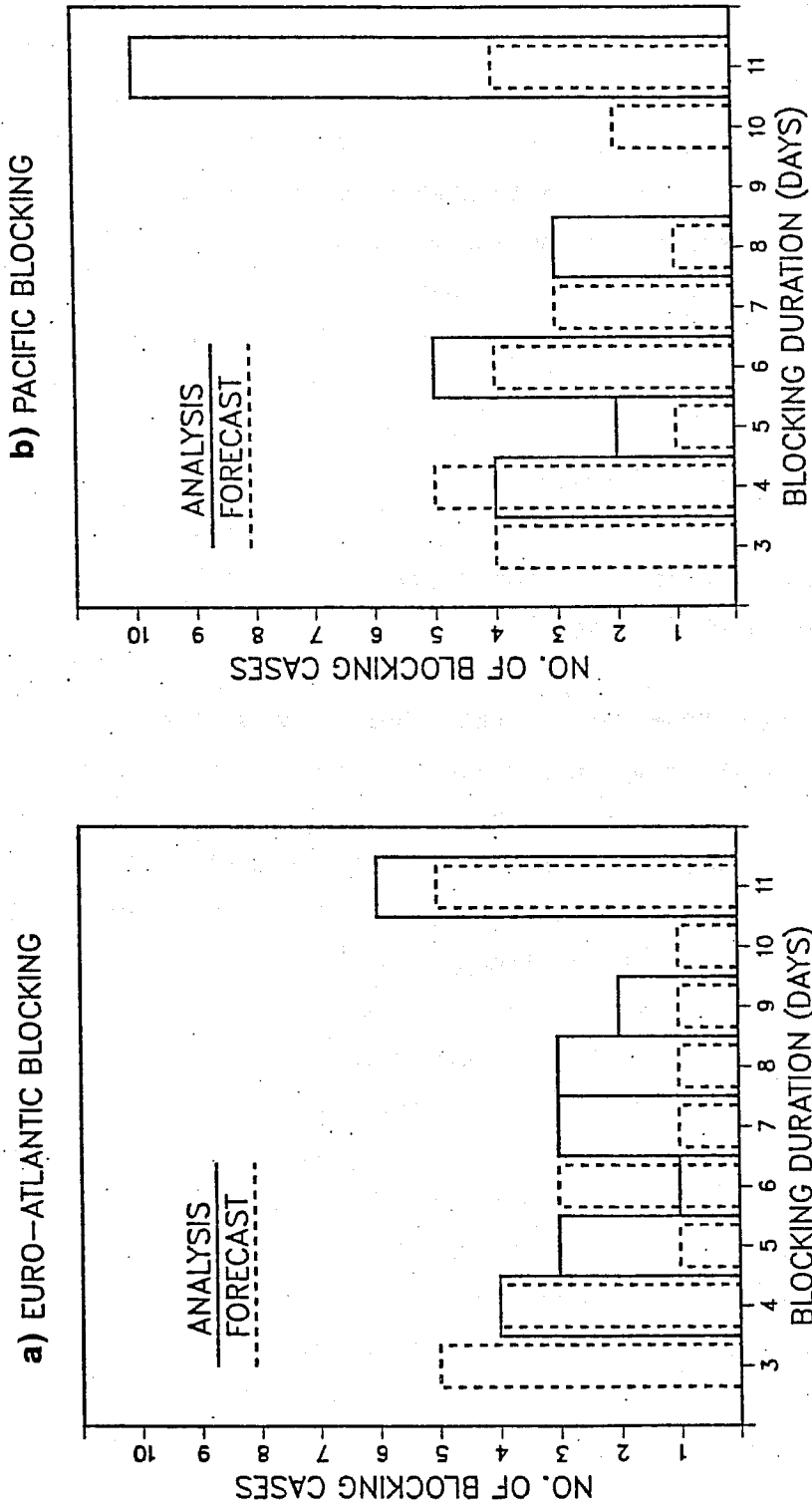


Fig. 15 Histograms of the number of blocking cases as a function of duration for the Euro-Atlantic (a) and the Pacific (b) sector.

6. MODEL SYSTEMATIC ERRORS AND BLOCKING

The problem of climate drift in General Circulation Models has long been recognized as one of major concern and has received much attention in recent years (for a few examples, see the works quoted at the beginning of Section 3). Our perception of model systematic error as a large (but seasonally homogeneous) ensemble mean of forecast error fields would have to be taken with caution if it could be shown with certainty that the distribution in phase space of possible atmospheric states is not unimodal. Since convincing evidence to this effect is accumulating (although not universally accepted as such; Sutera, 1986; Hansen, 1986; Hansen and Sutera, 1986; Benzi et al., 1986a) and since such atmospheric "modes" or "states" have been often associated to the blocking phenomenon, it is of particular interest to diagnose model systematic errors using blocked and non-blocked ensembles separately. To increase our sample as much as possible, we will return here to our instantaneous (i.e. based on daily maps) definition of blocked sectors, but before analysing model performance we want to look at analysed ensemble mean maps of our blocked "states".

Figure 16 shows five 500mb geopotential height maps. Panel (a) represents the "climate", that is the complete 700-day ensemble mean, (b) is the ensemble of the 278 non-blocked, or "zonal" days, (c) is the ensemble of the 422 blocked days, (d) is the ensemble of the 273 Euro-Atlantic blocked days and (e) of the 285 Pacific blocked days. Although full fields are usually dominated by the westerly main structure, it is already possible to recognize the essential features of the Rockies ridge (e), characteristic of the Pacific blocking and of the Eastern Atlantic diffluence region (d), characteristic of Euro Atlantic block. A better way to emphasize the structures we are most interest in is to show the three maps (c-b), (d-b) and (e-b), that is the "anomalies" computed not with respect to the full climate (a), but with respect to the zonal climate (b). These are shown in Figure 17, panels (a) to (c), while panels (d) to (f) show the eddy component of the same three maps, that is their departure from zonal mean. Now the blocking dipolar structures are quite evident in the respective quadrants. What was perhaps less obvious to expect is the signal appearing over the North American continent in both panels (e) and (f), another dipole structure of the opposite sign of the blocking dipole (negative to the north and positive to the south). Obviously, the definition of eddy field itself requires a compensation of the blocking dipoles in order

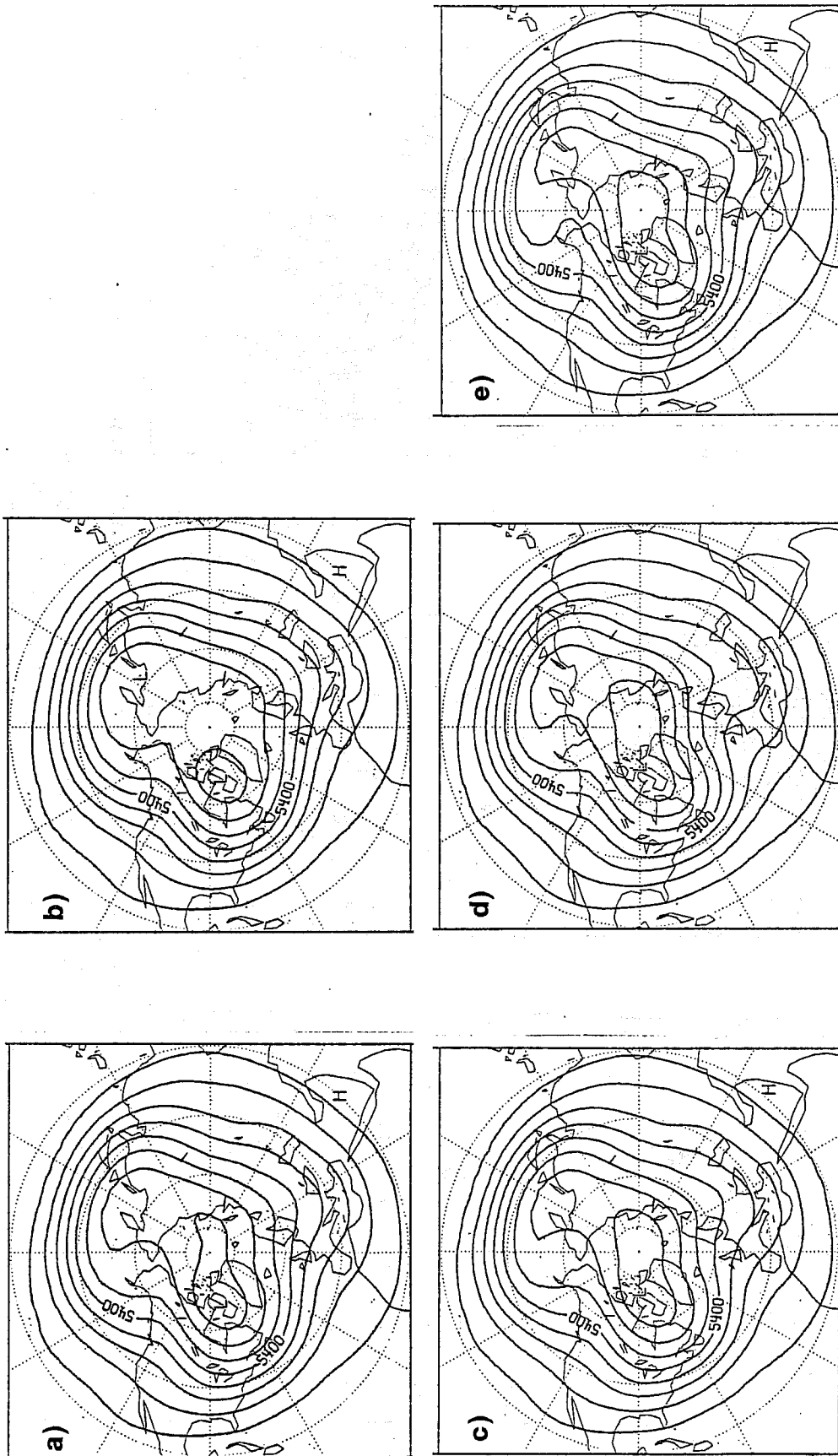


Fig. 16 Ensemble mean maps of 500mb geopotential height computed from (a) the complete 700-day sample; (b) the ensemble of the 278 non-blocked, or "zonal" days; (c) the ensemble of the 422 blocked days; (d) the ensemble of the 273 Euro-Atlantic blocked days; (e) the ensemble of the 285 Pacific blocked days.

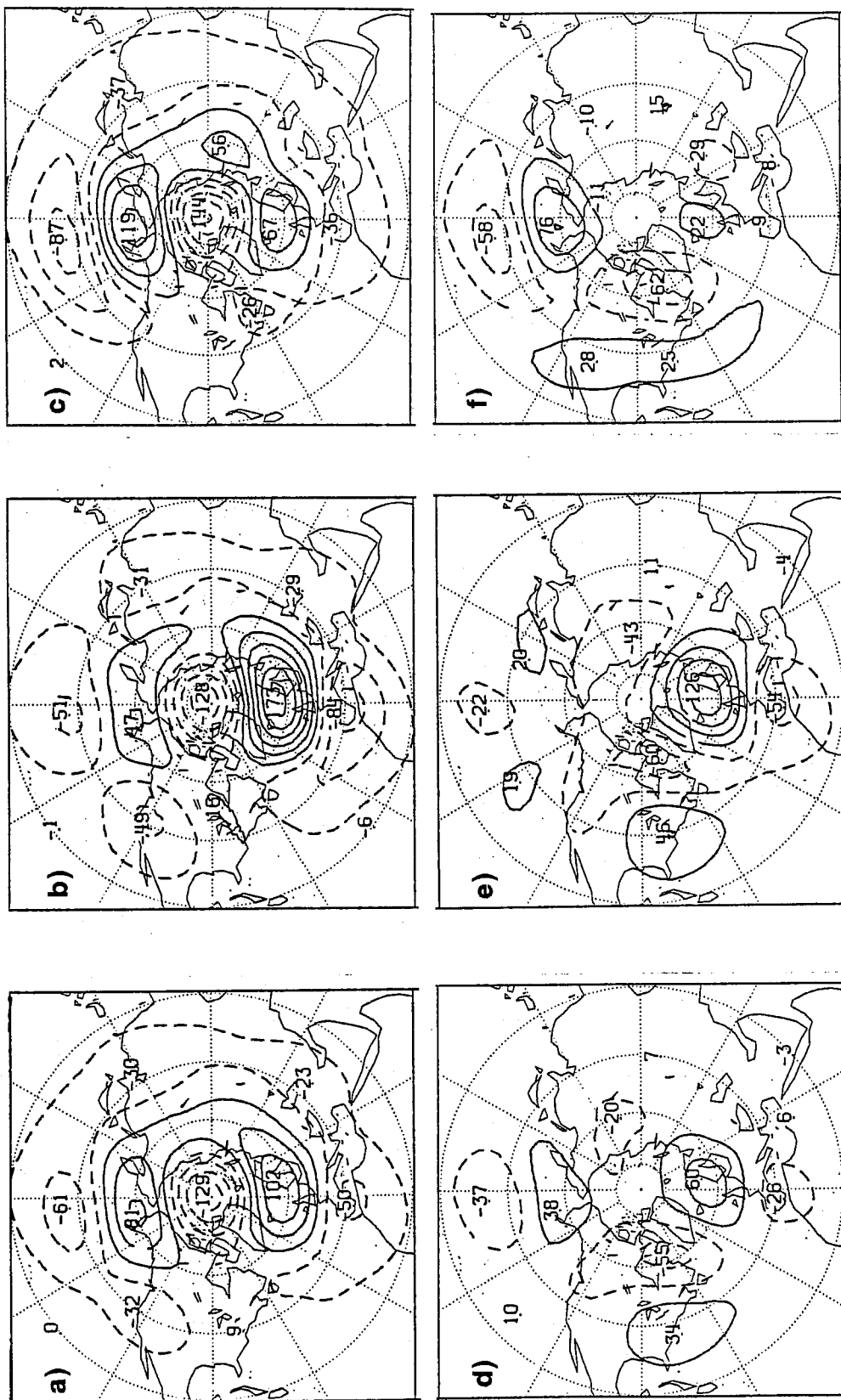


Fig. 17 (a) Difference between 'blocked' and 'zonal' ensemble maps
 (Fig. 16c-Fig. 16b).
 (b) as (a), but for Euro-Atlantic blocking (Fig. 16d-Fig. 16b).
 (c) as (a), but for Pacific blocking (Fig. 16e-Fig. 16b).
 (d), (e) and (f) as (a), (b), (c) respectively, but only showing the
 eddy component of the difference fields.

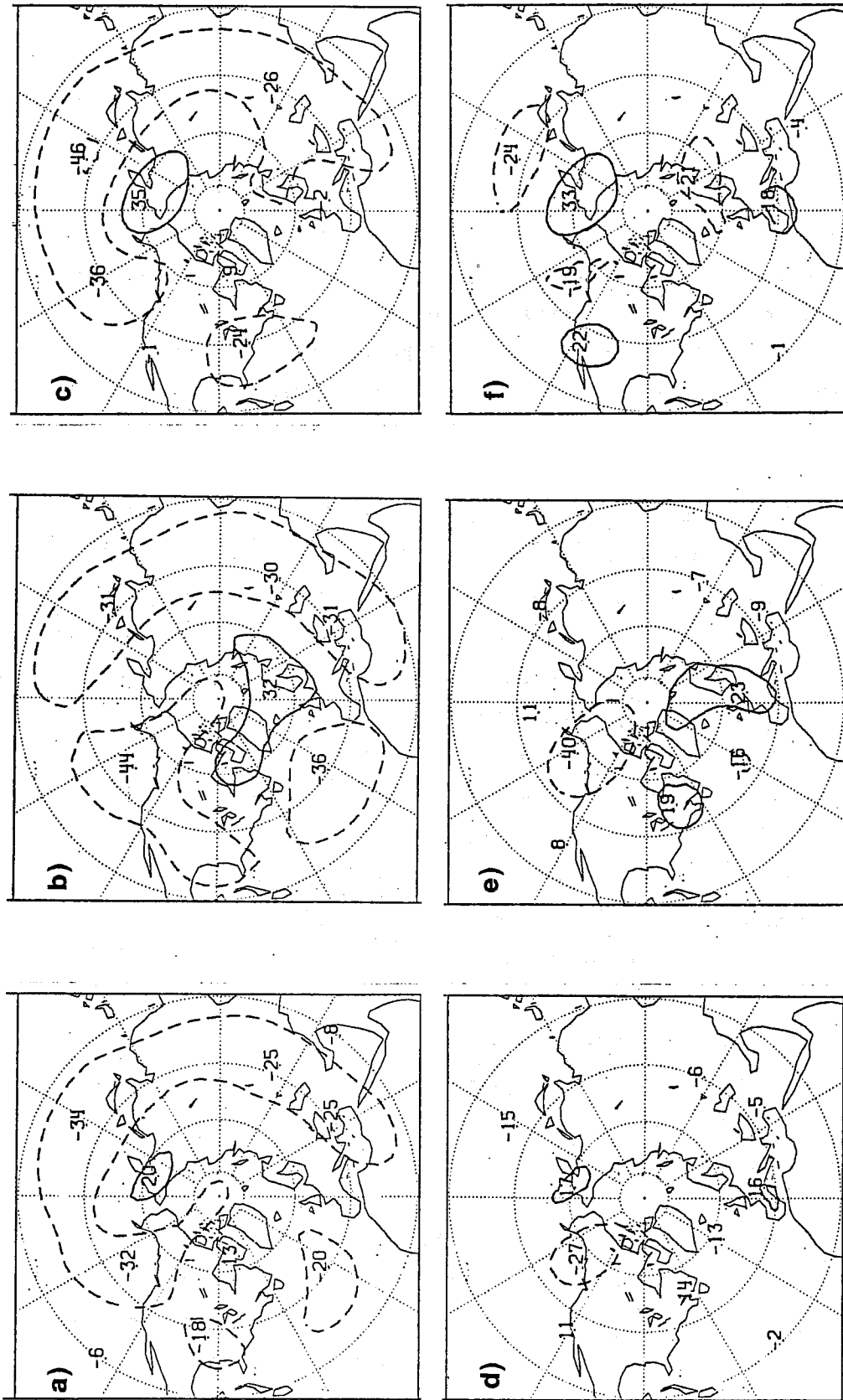


Fig. 18 As in Fig. 17 but deduced from ensemble means of 10-day forecast fields verifying on the same 'zonal' or 'blocked' days.

to obtain a zero-valued zonal mean. However, a priori there is no reason why these compensating features should be concentrated in a single region. In particular, one can note how a similar signal is completely absent from the Asian region.

We can now turn to model performance. Figure 18 is the exact counterpart of Fig. 17 but instead of being constructed using analysed fields, it was produced using 10 day forecast fields. The almost complete absence of significant structures is striking and even more so for the eddy-only part of the fields (panels d to f). Essentially, the inability of the model in representing the observed blocks is reflected by the absence, in the ensemble mean maps, of those structures that are the essential signature of the actual atmospheric process.

Figures 19 and 20 have the same essential layout as Fig 16, but instead of showing analysed ensemble means, they display day 10 forecast minus verifying analysis, that is the systematic error in the different atmospheric regimes. Fig. 19 shows the ensemble mean errors as full fields, while Fig 20 shows their departure from their own respective zonal means (the systematic error in the eddy field). A direct comparison respectively between Figs. 17 (b) and (c) and Figs. 19 (d) and (e) (full fields) and between Figs. 17 (e) and (f) and Figs. 20 (d) and (e) (eddy component) confirms that the systematic error signatures are almost equal and opposite in sign to those characteristic of blocking. This is nothing but a quantitatively more accurate restatement of the fact that the model, well into the medium range (day 10), is unable to enter and/or to maintain blocking at the observed levels. A comparison of Fig. 20 (b) with Figs. 20 (c), (d) and (e) reveals that, although the systematic error signature during non-blocked ("zonal") days is qualitatively not dissimilar to that characteristic of either Euro-Atlantic or Pacific blocking (essentially a structure dominated by zonal wavenumber two), its amplitude is quite different, and in fact much smaller. Further to this, Figure 21 shows the systematic error of the purely zonal part of the field (expressed in m/s of geostrophic wind as a function of latitude) during the different regimes. In this case, the systematic error during the blocked and non-blocked regimes is quite different (and the first dominates over the second in the total ensemble, see panel (a)). During zonal periods, the zonal systematic error (panel (b)) has the structure of a weak double band of

excessive westerlies, around 45°N and 80°N, with an even weaker easterly band in between. At low latitudes, the error is easterly again. This error structure implies a northward shift of both the subtropical and the polar branches of the jet. During blocking (either Euro-Atlantic or Pacific), the structure of the systematic error is the familiar one, so often and exhaustively documented in the literature (see again the works mentioned above, in Section 3), that is one of a strong northward displacement of the subtropical jet and of strong reduction of the westerlies at high latitudes. In other words, the model tends to cancel the split of the jet that occurs in the actual atmosphere.

We can conclude that the fact that blocking is associated with an enhancement of the amplitude of the quasi-stationary planetary scale waves (e.g. Austin, 1980; Hansen and Chen, 1982; Ji and Tibaldi, 1983), the fact that the model is unable to maintain the observed amplitude of the planetary waves beyond 3 to 4 days into the forecast and the fact that the model is also not capable of entering blocking beyond 3 to 4 days into the forecast are connected facts, although it is impossible at this stage to ascertain whether the third is a cause or a consequence of the second (via the first). We have, however, shown that the well known zonal and eddy signature of the model systematic error is mostly produced during blocked situation; it therefore reflects the inability of the model to exit the zonal state and to enter the blocked state. What is the ultimate (or at least, the principal) cause of this inability is still an open question; the answer strongly depends on the role that global and local dynamics play in the process of blocking onset.

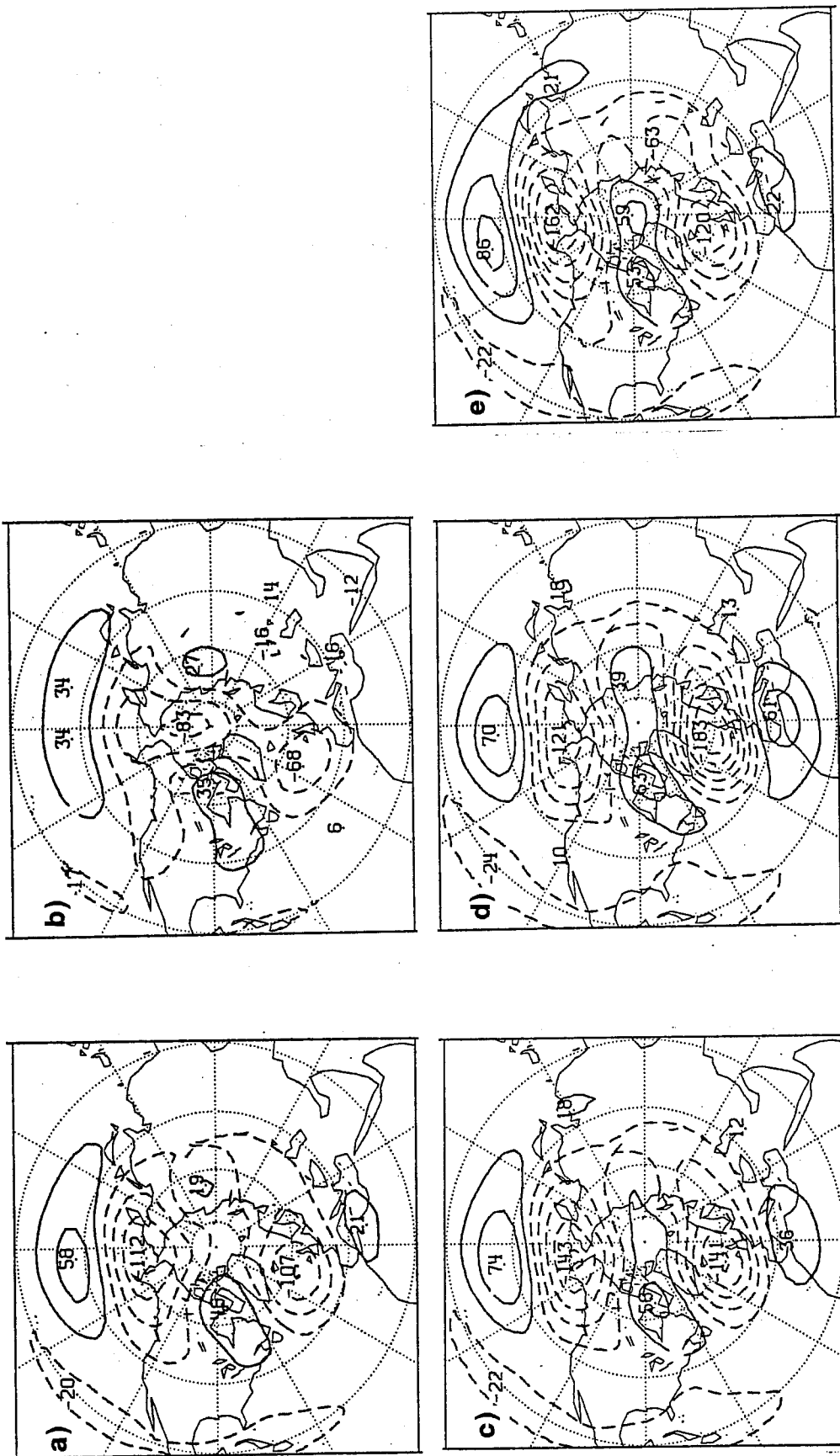


Fig. 19 As in Fig. 16, but for ensemble means of 500 mb height errors of 10-day forecasts.

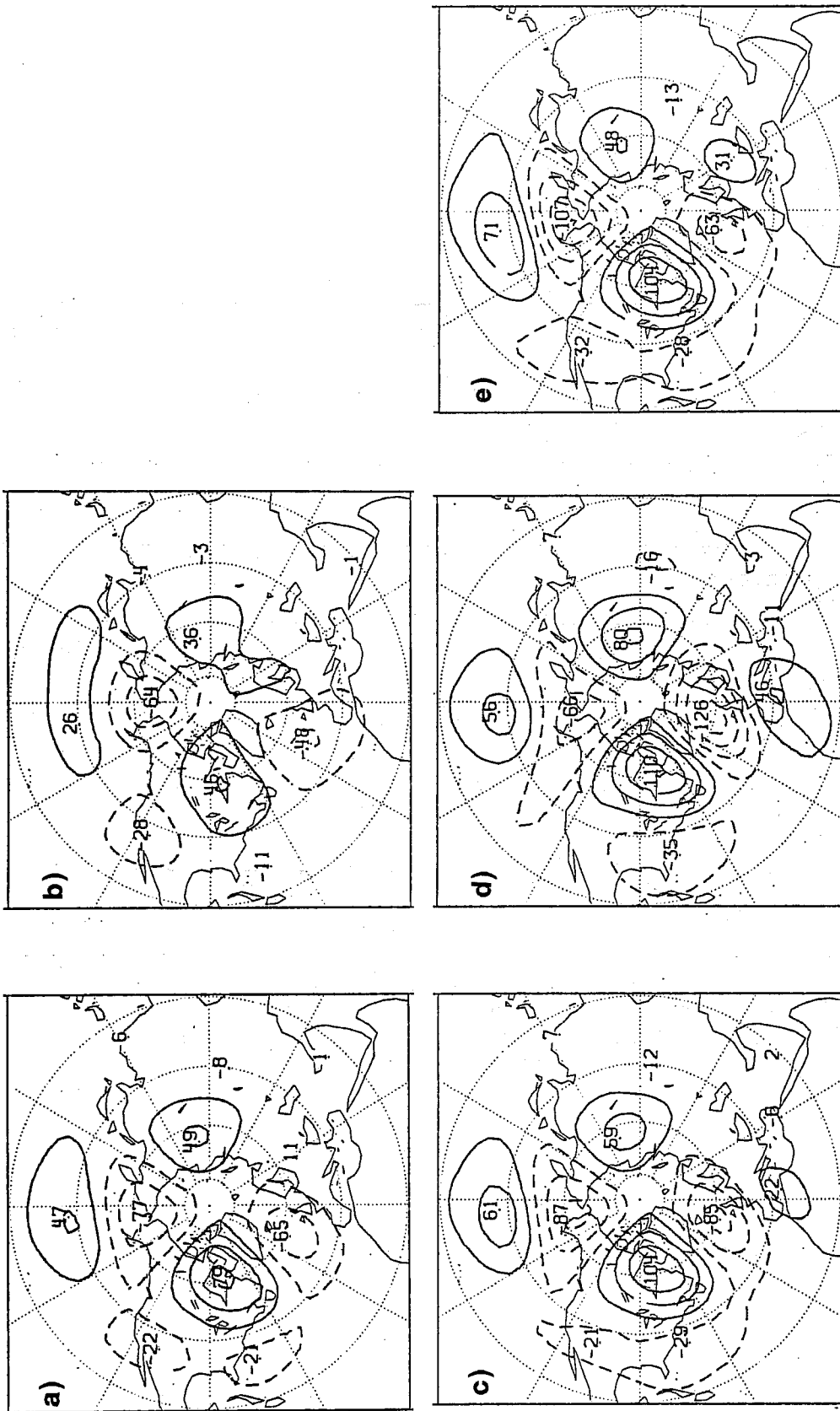


Fig. 20 As in Fig. 19, but only for the eddy component of the error fields.

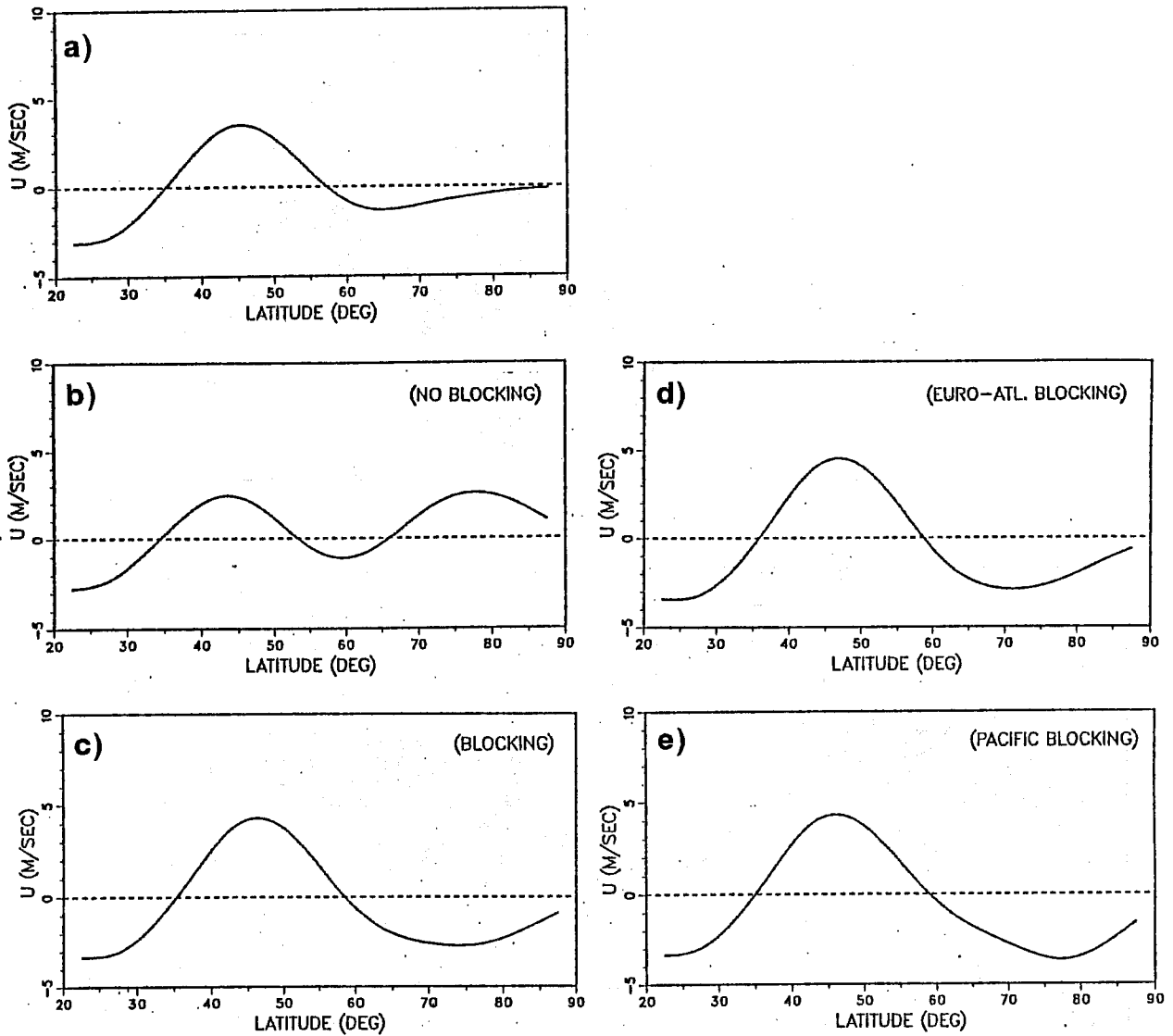


Fig. 21 Ensemble mean error of the zonally averaged geostrophic wind (in m/s) as a function of latitude. The correspondence between panels (a) to (e) and the 5 different ensembles is the same as in Fig. 16.

7. SUMMARY AND CONCLUSIONS

We have used seven 100 day winter periods (1980-81 to 1986-87) of ECMWF operational 500mb height analyses and forecasts (day 1 to 10) to assess the skill of the Centre's model in short and medium range forecast of blocking. Firstly we have given an objective definition of blocking (following essentially Lejenas and Okland, 1983) and we have diagnosed the behaviour of the model as a function of latitude and forecast day. We have also stratified the diagnosis for different two-year periods during which the model characteristics remained fairly stable. We then proceeded to distinguish between Euro-Atlantic and Pacific blocking by specifying an objective definition of "blocked sectors". In order to be able to analyse separately blocking onset and blocking maintenance, we further restricted our choice to episodes longer than three days (we found in this way 22 cases of Euro-Atlantic and 24 cases of Pacific blocking). We finally examined zonal and eddy components of model systematic errors during the so-defined circulation regimes.

On the basis of this diagnostic analysis we reached the following conclusions:

- a) Serious systematic deficiencies were found in the model simulation of blocking after forecast day 3 to 4: only about 50% of blocking days are found at forecast day 10 compared to the analysis, and approximately half of those do not correspond to actually observed blocked days.
- b) Only slight improvements were found in the model ability of reproducing blocking during the seven winters of operations analysed.
- c) Differences between Euro-Atlantic and Pacific blocking forecasts were found as far as improvement in forecast quality during the years (as model resolution and physics improved), phase and amplitude errors, and skill in predicting the duration of blocks are concerned. Such differences point towards different dominating mechanisms for the maintenance of long-lived blocking structures in the two different sectors.
- d) Blocking onset is almost consistently missed by the model beyond forecast day 3 to 4; conversely, once blocking appears in the initial

conditions, duration is reasonably well predicted into the medium range (although with some underestimation).

- e) Systematic model errors appear to be mainly produced by the inability of the model to represent the transition between "zonal" and blocked regimes. It would seem more appropriate to talk about a "systematic model regime" (the zonal one) rather than of a systematic model error. A promising avenue to follow in order to throw more light onto possible causes of systematic errors appears therefore to be the investigation of the physical mechanisms that cause the onset of blocking.

REFERENCES

Arpe, K. and E. Klinker, 1986: Systematic errors of the ECMWF operational forecasting model in mid-latitudes. *Quart.J.R.Met.Soc.*, 112, 181-202.

Austin, J.F., 1980: The blocking of middle latitude westerly winds by planetary waves. *Quart.J.R.Met.Soc.*, 106, 327-350.

Bengtsson, L., 1981: Numerical prediction of atmospheric blocking. A case study. *Tellus*, 33, 19-42.

Bengtsson, L., and A.J. Simmons, 1982: Medium range weather prediction - operational experience at ECMWF. In "Large-Scale Dynamical Processes in the Atmosphere". (B.J. Hoskins and R.P. Pearce, eds.) pp.337-363. Academic Press, New York.

Benzi, R., A. Speranza and A. Sutera, 1986a: A minimal baroclinic model for the statistical properties of low-frequency variability. *J.Atmos.Sci.*, 43, 2962-2967.

Benzi, R., P. Malguzzi, A. Speranza and A. Sutera, 1986b: The statistical properties of general atmospheric circulation: observational evidence and a minimal theory of bimodality. *Quart.J.R.Met.Soc.*, 112, 661-674.

Bettge, T.W., 1983: A systematic error comparison between the ECMWF and NMC prediction models. *Mon.Wea.Rev.*, 111, 2385-2389.

Charney, J.G., and J.G. DeVore, 1979: Multiple flow equilibria and blocking. *J.Atmos.Sci.*, 36, 1205-1216.

Charney, J.G., D.M. Strauss, 1980: Form-drag instability, multiple equilibria and propagating planetary waves in baroclinic, orographically forced, planetary wave system. *J.Atmos.Sci.*, 37, 1157-1175.

Dole, R.M. and N.D. Gordon, 1983: Persistent anomalies of the extratropical northern hemisphere wintertime circulation: geographical distribution and regional persistence characteristics. *Mon.Wea.Rev.*, 111, 1567-1586.

Green, J.S.A., 1977: The weather during July 1976: some dynamical considerations of the drought. *Weather*, 32, 120-128.

Grønnaas, S., 1982: Systematic errors and forecast quality of ECMWF forecasts in different large-scale flow patterns. ECMWF Seminar/Workshop on Interpretation of Numerical Weather Prediction Products, 13-24 September 1982. ECMWF, Shinfield Park, Reading, UK., 161-206.

Hansen, A.R., 1986: Observational characteristics of atmospheric planetary waves with bimodal amplitude distribution. *Advances in Geophysics*, 29, 101-133.

Hansen, A.R. and T.C. Chen, 1982: A spectral energetics analysis of atmospheric blocking. *Mon.Wea.Rev.*, 110, 1146-1165.

Hansen, A.R. and A. Sutera, 1986: On the probability density distribution of planetary-scale atmospheric wave amplitude. *J.Atmos.Sci.*, 43, 3250-3265.

- Hollingsworth, A., K. Arpe, M. Tiedtke, M. Capaldo, and H. Savijarvi, 1980: The performance of a medium-range forecast model, in winter - impact of physical parameterizations. *Mon.Wea.Rev.* 108, 1736-1773.
- Hollingsworth, A., U. Cubasch, S. Tibaldi, C. Brankovic, T.N. Palmer and L. Campbell, 1987: Mid-latitude atmospheric prediction on time scales of 10-30 days. pp 117-151 in *Atmospheric and Oceanic Variability*, Ed. H. Cattle. Royal Meteorological Society, Bracknell.
- Hoskins, B.J. and P.D. Sardeshmukh, 1987: A diagnostic study of the dynamics of the northern hemisphere winter of 1985/86. *Q.J.R. Meteorol.Soc.*, 113, 759-778.
- Illari, L., and J.C. Marshall, 1983: On the interpretation of eddy fluxes during a blocking episode. *J.Atmos.Sci.*, 40, 2232-2242.
- Ji, L.R. and S. Tibaldi, 1983: Numerical simulations of a case of blocking: The effects of orography and land-sea contrast. *Mon.Wea.Rev.*, 111, 2068-2086.
- Källén, E. 1981: Bifurcation properties of quasi-geostrophic, barotropic models and their relation to atmospheric blocking. *Tellus*, 34, 255-265.
- Lau, N.-C., 1983: Mid-latitude wintertime circulation anomalies appearing in a 15-year GCM experiment. pp 111-125 in *Large-Scale Dynamical Processes in the atmosphere*, Eds. B.J. Hoskins and R.P. Pearce, Academic Press, New York.
- Lejenäs, H. and Økland, H., 1983: Characteristics of Northern Hemisphere blocking as determined from a long time series of observational data. *Tellus*, 35A, 350-362.
- Lorenz, E., 1982: Atmospheric predictability experiments with a large numerical model. *Tellus*, 34A, 505-513.
- Malguzzi, P. and A. Speranza, 1981: Local multiple equilibria and regional atmospheric blocking. *J.Atmos.Sci.*, 38, 1939-1948.
- Mansfield, D.A., 1984: The incidence of blocking in the Meteorological Office 5-level model. *Met. 013 Branch Memo. No. 99*. Available from U.K. Meteorological Office, Bracknell.
- Palmer, T.N., G.J. Shutts and R. Swinbank, 1986: Alleviation of a systematic westerly bias in general circulation and numerical weather prediction models through an orographic gravity wave drag parametrization. *Quart.J.R.Met.Soc.*, 112, 1001-1039.
- Rex, D.R., 1950: Blocking action in the middle troposphere and its effect upon regional climate. II: The climatology of blocking actions. *Tellus*, 2, 275-302.
- Shutts, G.J., 1986: A case study of eddy forcing during an Atlantic blocking episode. *Advances in Geophysics*, 29, 135-164.
- Speranza, A., 1986: Deterministic and statistical properties of northern hemisphere middle latitude circulation: minimal theoretical models. *Advances in Geophysics*, 29, 199-266.

Sutera, A., 1986: Probability density distribution of large scale atmospheric flow. *Advances in Geophysics*, 29, 319-338.

Tibaldi, S., C. Brankovic and U. Cubasch, 1987: 30-day integrations using the operational ECMWF spectral model. ECMWF Tech.Memo. No. 138. Available from ECMWF, Reading.

Wallace, J.M., S. Tibaldi, and A.J. Simmons, 1983: Reduction of systematic forecast errors in the ECMWF model through the introduction of an envelope orography. *Quart.J.R.Met.Soc.*, 109, 683-717.